

# Polyakov loops, Gross-Witten like point and Hagedorn states

I. Zakout and C. Greiner

*Institut für Theoretische Physik, J. W. Goethe-Universität,*

*D-60438 Frankfurt am Main, Germany*

(Dated: July 28, 2011)

## Abstract

The phase transition for a finite volume system that incorporates the Polyakov loops and maintains the colorless state is explored using the Polyakov-loop extended Nambu-Jona-Lasinio (PNJL) model. The order parameter for Polyakov loops is demonstrated to signal the appearance of a transition for  $SU(3)_c$  analogous to Gross-Witten (GW-) phase transition instead of the deconfinement phase transition to quark-gluon plasma. The asymptotic restoration of Polyakov loops is conjectured to be a threshold production for meta-stable Hagedorn (or semi-QGP) states and this does not imply a direct deconfinement phase transition. In this context, the GW-like point is the point where the colorless states switches from the low-lying hadronic states to the meta-stable high-lying Hagedorn states. The chiral phase transition takes place within an extended GW-like point depending on the fireball's size. The deconfinement phase transition is determined by Hagedorn's temperature above GW-like temperature.

## I. INTRODUCTION

Recently, Fukushima [1] has extended the Nambu-Jona-Lasinio (NJL) model to include Polyakov loops, namely,  $\Phi$  and  $\bar{\Phi}$  and the  $\sigma$ -chiral field. Fukushima's approach is known as Polyakov extended Nambu-Jona-Lasinio (PNJL) model. The Polyakov loops are related to the imposition of the Gauss' law where the trivial vacuum is a minimum of the free energy and the formation of stable colorless QG-droplet [2]. The PNJL model has been widely adopted to study the phase transition diagram. Furthermore, it has been extended to investigate the phase transition diagram with various phenomenological effective Polyakov and gluon potentials as well as various extensions to include other NJL's fields such as the isospin scalar and vector fields as well as the color superconductivity [1, 3–13]. The hybrid description of PNJL with two and three flavors has been studied extensively with various modifications of the effective Polyakov and gluon potential and the results have been compared with lattice QCD data [4]. The Polyakov potential as a function of Polyakov loops (or equivalently the VanderMonde potential as a function of fundamental eigenvalues of the Gauss-law) is originated from the invariance Haar measure of  $SU(N_c)$  in order to project the colorless state of the quark and gluon fireball. The comparison with lattice calculations [3, 4, 6, 8] hints that the effective Polyakov potential could be modified by temperature. Furthermore, it has been suggested that modifying the invariance Haar measure's exponent somehow mutates the Hagedorn's internal structure [14]. Furthermore, the bag's volume fluctuation can modify the effective Polyakov potential. Nevertheless, the modification of the effective Polyakov potential in the medium and its impacts in the phase transition diagram will be considered in a future work. The internal structure of the quark-gluon (QG) has been suggested to be crucial to the tri-critical point (see for instance Ref. [15] and reference therein). This has a significant impact in the recent research to explore the width of phase transition and intermediate processes such as Hagedorn states, quarkyonic matter and semi-classical QGP phases and color-flavor superconductor matter. There exist various reviews discussing the QG-blob's internal color structure. Brezin, Itzykson, Parisi and Zuber studied the planar approximation to field theory through the limit of a large internal symmetry group [16]. This procedure is known as the matrix saddle point method. Gross and Witten [17] using the matrix method have discovered a possible transition from a specific phase with strong coupling to another phase with weak coupling in the large  $N_c$  limit (i.e.  $N_c \rightarrow \infty$ ).

but a finite  $g^2 N_c$ ) of Wilson lattice gauge theory. For technical reasons, the spectral density method which has been developed by Brezin *et. al.* [16, 17] depends basically on the large  $N_c$  limit and it is not permissible for technical reasons to extend the same analyses using the spectral density for finite number of colors. The GW-like point sticks in one's mind for  $N_c \rightarrow \infty$  and remains obsolete for  $N_c = 3$  (i.e. the QCD). The GW-like phase transition for finite  $N_c$  is not expected to have the same characteristic behavior to that one in the limit  $N_c \rightarrow \infty$ . In order to search for a mechanism analogous to GW-transition in QCD, it is important to extend the analysis using the (non-Gaussian-) stationary points method in the strong coupling limit in the context of the Polyakov loop parameterization as done by in Ref [1] and the references therein on one hand and the (Gaussian-) saddle points approximation in the weak coupling limit as done by Elze, Greiner and Rafelski and others [18–28] on the other hand. The interpolation between the asymptotic non-Gaussian stationary points approximation's solution for the strong coupling limit and the asymptotic Gaussian saddle points approximation's solution for the weak coupling limit is not fully understood in QCD and the corresponding mechanism is analogous to GW-transition. Furthermore, GW-like transition sounds to take place over the interpolation range between two asymptotic solutions (i.e. over an extended interval) rather than a single deflection point. Furthermore, Elze, Greiner and Rafelski have pointed out that the non-perturbative effect of the colorless state leads to a gradual freezing of internal degrees of freedom [20, 21]. This mechanism could explain the emergence of QG liquid droplet(s) or equivalent forms such as Hagedorn states, quarkyonic droplets etc. It should be stressed that GW-like transition is not a confinement/deconfinement phase transition, but instead is the production threshold of (meta-) Hagedorn states in hadronic matter. The Hagedorn states emerge as gas of bags. Therefore, there is a possibility for a new form of matter that can be formed in a narrow range above GW-like point and below Hagedorn's temperature. This form of matter emerges as a gas/liquid of bags and these bags expand and grow up gradually. When Hagedorn's temperature is reached, the system undergoes a deconfinement phase transition to QGP.

The outline of the present paper is as follows: In Sec. II, we review Polyakov loops without chiral field and demonstrate the interpolation between the low-lying and high-lying energy solutions and a possible transition that is analogous to GW-transition. In Sec. III, the treatment is extended to include the  $\sigma$ -chiral field in the context of PNJL model and

demonstrate the emergence of an extended GW-like point. The connection between GW-like point and production of Hagedorn states is discussed in Sect. IV. Finally, the conclusion is presented in Sec. V.

## II. A SIMPLE CANONICAL ENSEMBLE WITH POLYAKOV LOOPS

The grand potential for the quark and the anti-quark is given by

$$\begin{aligned} \frac{\Omega_{q\bar{q}}(\beta, V; \theta_1, \theta_2)}{V} &= -\frac{1}{V\beta} \log_e Z_{q\bar{q}}(\beta, V; \theta_1, \theta_2), \\ &= -(2J+1) \sum_q \int \frac{d^3\vec{p}}{(2\pi)^3} \sum_i^{N_c} \left[ \epsilon_q(\vec{p}) + \frac{1}{\beta} \log_e \left( 1 + e^{-\beta[\epsilon_q(\vec{p}) - \mu_q - i\frac{\theta_i}{\beta}]} \right) \right. \\ &\quad \left. + \frac{1}{\beta} \log_e \left( 1 + e^{-\beta[\epsilon_q(\vec{p}) + \mu_q + i\frac{\theta_i}{\beta}]} \right) \right], \end{aligned} \quad (1)$$

where  $\epsilon_q(\vec{p}) = \sqrt{\vec{p}^2 + m_q^2}$ ,  $(2J+1) = 2$  is the spin degeneracy,  $V$  is the quark and gluon blob's volume and  $\mu_q$  is the flavor chemical potential while  $\theta_i$  are the imaginary color chemical potentials or fundamental gauge fields of the  $SU(N_c)$  group's fundamental representation (i.e. Gauss-law's eigenvalues on the thermal excitations). When no chiral fields are involved in the calculation,  $m_q$  is reduced to the current mass (for only the sake of simplicity, it can be assumed massless for light flavors). The first term in the square bracket that appears on the right hand side of Eq.(1) is temperature independent. It diverges at zero temperature and is a non-re-normalizable term. It can be regulated in the standard way by introducing UV-cutoff for the momentum integration. In the standard  $\sigma$ -model, that term is trivially dropped as far it can be absorbed by the nonlinear  $\sigma$ -potential but the this is not the case in Nambu-Jona-Lasinio model (NJL) where the first term is regularized and retained in the calculation. After a simple algebraic manipulation, Eq.(1) becomes

$$\begin{aligned} \frac{\Omega_{q\bar{q}}(\beta, V; \Phi, \bar{\Phi})}{V} &= \frac{\Omega_{q\bar{q}}(\beta, V; \theta_1, \theta_2)}{V}, \\ &= -2N_c \sum_q \int_0^\Lambda \frac{d|\vec{p}| |\vec{p}|^2}{2\pi^2} \epsilon_q(\vec{p}) \\ &\quad - \frac{2}{\beta} \sum_q \int \frac{d^3\vec{p}}{(2\pi)^3} \\ &\quad \times \left( \log_e \left[ 1 + 3 \left( \Phi + \bar{\Phi} e^{-\beta[\epsilon_q(\vec{p}) - \mu_q]} \right) e^{-\beta[\epsilon_q(\vec{p}) - \mu_q]} + e^{-3\beta[\epsilon_q(\vec{p}) - \mu_q]} \right] \right. \\ &\quad \left. + \log_e \left[ 1 + 3 \left( \bar{\Phi} + \Phi e^{-\beta[\epsilon_q(\vec{p}) + \mu_q]} \right) e^{-\beta[\epsilon_q(\vec{p}) + \mu_q]} + e^{-3\beta[\epsilon_q(\vec{p}) + \mu_q]} \right] \right), \end{aligned} \quad (2)$$

where  $\Lambda$  is UV-cutoff that regularizing the divergent term over the momentum integration. The UV-cutoff for momentum integration is taken  $\Lambda = 631.5$  MeV in the present calculations. The Polyakov-loop triality parameters  $\Phi$  and  $\bar{\Phi}$  are defined, respectively, as follows

$$\begin{aligned}\Phi &= \frac{1}{N_c} [e^{i\theta_1} + e^{i\theta_2} + e^{i\theta_3}], \\ \bar{\Phi} &= \frac{1}{N_c} [e^{-i\theta_1} + e^{-i\theta_2} + e^{-i\theta_3}],\end{aligned}\quad (3)$$

where  $\theta_3 = -\theta_1 - \theta_2$  for  $SU(3)_c$  and the fundamental gauge fields  $\theta_i, i = 1, 2, 3$  are subjected to the periodicity condition over the interval  $-\pi \leq \theta_i \leq \pi$ . Eq.(2) can be written as follows

$$\begin{aligned}\frac{\Omega_{q\bar{q}}(\beta, V; \Phi, \bar{\Phi})}{V} &= -2N_c \sum_q \int_0^\Lambda \frac{d|\vec{p}| |\vec{p}|^2}{2\pi^2} \epsilon_q(\vec{p}) \\ &\quad - 6 \sum_q \int \frac{d|\vec{p}|}{(2\pi^2)} \frac{|\vec{p}|^4}{3\epsilon_q(\vec{p})} \\ &\quad \times \left( \frac{(\Phi + 2\bar{\Phi}e^{-\beta[\epsilon_q(\vec{p})-\mu_q]}) e^{-\beta[\epsilon_q(\vec{p})-\mu_q]} + e^{-3\beta[\epsilon_q(\vec{p})-\mu_q]}}{1 + 3(\Phi + \bar{\Phi}e^{-\beta[\epsilon_q(\vec{p})-\mu_q]}) e^{-\beta[\epsilon_q(\vec{p})-\mu_q]} + e^{-3\beta[\epsilon_q(\vec{p})-\mu_q]}} \right. \\ &\quad \left. + \frac{(\bar{\Phi} + 2\Phi e^{-\beta[\epsilon_q(\vec{p})+\mu_q]}) e^{-\beta[\epsilon_q(\vec{p})+\mu_q]} + e^{-3\beta[\epsilon_q(\vec{p})+\mu_q]}}{1 + 3(\bar{\Phi} + \Phi e^{-\beta[\epsilon_q(\vec{p})+\mu_q]}) e^{-\beta[\epsilon_q(\vec{p})+\mu_q]} + e^{-3\beta[\epsilon_q(\vec{p})+\mu_q]}} \right). \quad (4)\end{aligned}$$

In the case of massless flavors and  $\mu_q = 0$  and in the terms of fundamental gauge fields, Eq.(4) reads

$$\begin{aligned}-\frac{\Omega_{q\bar{q}}(\beta, V; \Phi, \bar{\Phi})}{V} &= -\frac{\Omega_{q\bar{q}}(\beta, V; \Phi(\theta_1, \theta_2), \bar{\Phi}(\theta_1, \theta_2))}{V}, \\ &= -\frac{\Omega_{q\bar{q}}(\beta, V; \theta_1, \theta_2)}{V}, \\ &= \frac{\Lambda^4}{4\pi^2} N_f N_c + \frac{7\pi^2}{180\beta^4} N_f N_c - \frac{1}{6\beta^4} N_f \sum_{i=1}^{N_c} \theta_i^2 \left(1 - \frac{\theta_i^2}{2\pi^2}\right). \quad (5)\end{aligned}$$

The canonical ensemble for the quark and anti-quark becomes

$$Z_{q\bar{q}}(\beta, V; \Phi, \bar{\Phi}) = \exp[-\beta \Re \Omega_{q\bar{q}}(\beta, V; \Phi, \bar{\Phi})], \quad (6)$$

where  $\Omega_{q\bar{q}}(\beta, V; \Phi, \bar{\Phi})$  is given by Eq.(4). Fortunately, the  $q\bar{q}$  grand potential becomes a real one when  $\mu_q = 0$ . The partition function for the gluons can be calculated in a similar manner. The phenomenological gluon potential parameterized in the terms of Polyakov loops has been adopted recently in the literature [1]. The general choice is given by

$$\begin{aligned}\frac{1}{V} \Omega_g(\beta, V; \Phi, \bar{\Phi}) &= -\frac{1}{V} \frac{1}{\beta} \log_e Z_g(\beta, V; \Phi, \bar{\Phi}), \\ &= -2 \frac{1}{\beta^4} \left( \frac{a(T)}{4} \right) \bar{\Phi} \Phi,\end{aligned}\quad (7)$$

where Polyakov term  $\bar{\Phi}\Phi$  can be written in the terms of fundamental gauge fields as follows

$$\bar{\Phi}\Phi = \frac{1}{N_c^2} \sum_{i,j=1}^{N_c} \cos(\theta_i - \theta_j), \quad (8)$$

and

$$a(T) = a_0 + a_1 \left(\frac{T_0}{T}\right) + a_2 \left(\frac{T_0}{T}\right)^2, \quad (9)$$

where  $a_0$ ,  $a_1$  and  $a_2$  are phenomenological parameters. The phenomenological gluon partition function is usually adopted in the term of Polyakov loop approach in order to replace the standard gluon partition function that is given by

$$\begin{aligned} Z_g(\beta, V; \theta_1, \theta_2) &= \exp \left[ -2V \int \frac{d^3\vec{p}}{(2\pi)^3} \sum_{a=1}^{N_c^2-1} \log_e (1 - e^{-(\beta \epsilon_g(\vec{p}) - i\phi^a)}) \right], \\ &= \exp \left[ -2V \int \frac{d^3\vec{p}}{(2\pi)^3} \sum_i^{N_c} \sum_j^{N_c} \log_e (1 - e^{-(\beta \epsilon_g(\vec{p}) - i(\theta_i - \theta_j))}) \right], \end{aligned} \quad (10)$$

where  $\epsilon_g(\vec{p}) = |\vec{p}|$ . Eq.(10) is evaluated explicitly as follows

$$\log_e Z_g(\beta, V; \theta_1, \theta_2) = \frac{2V}{\beta^3} \left[ (N_c^2 - 1) \frac{\pi^2}{90} - \frac{1}{6} \sum_{i < j}^{N_c} (\theta_i - \theta_j)^2 \left( 1 - \frac{|\theta_i - \theta_j|}{2\pi} \right)^2 \right]. \quad (11)$$

In the standard treatment the gluons are treated as the adjoint interaction particles of the  $SU(N_c)$  symmetry group. It should be noted here that the  $SU(N_c)$ 's adjoint eigenvalues (i.e. adjoint gauge fields), namely,  $\phi^a$  are calculated from the nested commutation relations for the fundamental eigenvalues, namely,  $\theta_i$  of the Lie algebra. The adjoint eigenvalues are related to fundamental eigenvalues by the relation  $\phi^a \equiv (\theta_i - \theta_j)$ . This relation diagonalizes the adjoint representation and subsequently commutes with the Hamiltonian. In order to understand the origin of the gluon's phenomenological potential, Eq.(10) can be approximated and simplified in order to be evaluated using Polyakov loop variables in the following systematic way

$$\begin{aligned} Z_g(\beta, V; \Phi, \bar{\Phi}) &\approx \exp \left[ 2V\beta \sum_{a=1}^{N_c^2-1} \int \frac{d|\vec{p}|}{2\pi^2} \frac{|\vec{p}|^3}{3} \frac{1}{e^{i\phi^a} e^{\beta|\vec{p}|} - 1} \right], \\ &= \exp \left[ -2V\beta \int \frac{d|\vec{p}|}{2\pi^2} \frac{|\vec{p}|^3}{3} \frac{\sum_{n=1}^8 n C_n e^{-n\beta|\vec{p}|}}{1 + \sum_{n=1}^8 C_n e^{-n\beta|\vec{p}|}} \right], \end{aligned} \quad (12)$$

where the factor 2 that appears on the right hand side comes from the spin degeneracy. The coefficients  $C_n$  are functions of Polyakov loops [32]. When the Polyakov loops vanish ( $\Phi, \bar{\Phi} \rightarrow 0$ ), the gluon grand potential is reduced to  $\lim_{\Phi, \bar{\Phi} \rightarrow 0} \frac{1}{V} \Omega_g(\beta, V; \Phi, \bar{\Phi}) = -\frac{1}{\beta^4} \frac{1}{N_c^2} \frac{(N_c^2-1)\pi^2}{45}$ , while in the case of Polyakov loop restoration ( $\Phi, \bar{\Phi} \rightarrow 1$ ), it is reduced to  $\lim_{\Phi, \bar{\Phi} \rightarrow 1} \frac{1}{V} \Omega_g(\beta, V; \Phi, \bar{\Phi}) = -\frac{1}{\beta^4} \frac{(N_c^2-1)\pi^2}{45}$ . This implies that  $\Omega_g$  is reduced by factor  $1/N_c^2$  when  $\Phi, \bar{\Phi}$  are changed from 1 to 0. It can be parameterized to  $\frac{1}{V} \Omega_g(\beta, V; \Phi, \bar{\Phi}) \approx -\frac{1}{\beta^4} \frac{[(N_c^2-1)\Phi\bar{\Phi}+1]}{N_c^2} \frac{(N_c^2-1)\pi^2}{45}$ . In order to simplify the calculation drastically, the gluon grand potential is simplified to a phenomenological potential such as that one given in Eq.(7) as follows

$$\begin{aligned} \frac{1}{V} \Omega_g(\beta, V; \Phi, \bar{\Phi}) &\equiv -\frac{1}{\beta^4} \omega_g \bar{\Phi} \Phi, \\ &= -\frac{1}{\beta^4} \omega_g \frac{1}{N_c^2} \left[ 3 + 2 \sum_{i < j}^{N_c} \cos(\theta_i - \theta_j) \right], \end{aligned} \quad (13)$$

where

$$\omega_g = (N_c^2 - 1) \frac{\pi^2}{45}. \quad (14)$$

In the calculation of the phase transition from the low-lying energy excitations to the high-lying ones but below the deconfinement phase transition, it is adequate to use the potential that is given by Eq.(13).

The canonical ensemble for a finite volume quark and gluon blob in the Hilbert space is given by the Fock product of quark and antiquark partition function and the gluon partition function as follows

$$\begin{aligned} Z_{q\bar{q}g}(\beta, V; \theta_1, \theta_2) &= Z_{q\bar{q}g}(\beta, V; \theta_1, \theta_2, \theta_3 = -\theta_1 - \theta_2), \\ &= Z_{q\bar{q}g}(\beta, V; \Phi(\theta_1, \theta_1), \bar{\Phi}(\theta_1, \theta_1)), \\ &= Z_{q\bar{q}}(\beta, V; \Phi, \bar{\Phi}) \times Z_g(\beta, V; \Phi, \bar{\Phi}). \end{aligned} \quad (15)$$

This implies that the grand canonical ensemble is reduced to

$$\begin{aligned} Z_{q\bar{q}g}(\beta, V; \Phi, \bar{\Phi}) &= \exp(-\beta \Omega_{q\bar{q}g}(\beta, V; \Phi, \bar{\Phi})), \\ &= \exp(-\beta \Omega_{q\bar{q}g}(\beta, V; \theta_1, \theta_2)), \end{aligned} \quad (16)$$

where

$$\Omega_{q\bar{q}g}(\beta, V; \Phi, \bar{\Phi}) = \Re \Omega_{q\bar{q}}(\beta, V; \Phi, \bar{\Phi}) + \Omega_g(\beta, V; \Phi, \bar{\Phi}). \quad (17)$$

The colorless state for the quark and gluon blob is ensured by projecting the color singlet state in the following way

$$\begin{aligned}
Z_{colorless}(\beta, V) &= \int d\mu(\mathbf{g}) e^{\beta \Omega_{q\bar{q}g}(\beta, V; \Phi, \bar{\Phi})}, \\
&= \frac{1}{N!} \prod_{k=1}^{N_c-1} \left( \int_{-\pi}^{\pi} \frac{d\theta_k}{2\pi} \right) e^{-\beta \mathcal{V}_{VdM}(\mathbf{g})} Z_{q\bar{q}g}(\beta, V; \Phi, \bar{\Phi}), \\
&= \frac{1}{N!} \prod_{k=1}^{N_c-1} \left( \int_{-\pi}^{\pi} \frac{d\theta_k}{2\pi} \right) e^{-\beta [\mathcal{V}_{VdM}(\mathbf{g}) + \Omega_{q\bar{q}g}(\beta, V; \Phi, \bar{\Phi})]}, \tag{18}
\end{aligned}$$

where

$$\begin{aligned}
\int d\mu(\mathbf{g}) &= \frac{1}{N_c!} \frac{1}{(2\pi)^2} \int_{-\pi}^{\pi} d\theta_1 \int_{-\pi}^{\pi} d\theta_2 \int_{-\pi}^{\pi} d\theta_3 \delta \left( \sum_{i=1}^{3_c} \theta_i \right) \prod_{i < j} \left| 2 \sin \left( \frac{\theta_i - \theta_j}{2} \right) \right|^2, \\
&= \frac{1}{N_c!} \frac{1}{(2\pi)^2} \int_{-\pi}^{\pi} d\theta_1 \int_{-\pi}^{\pi} d\theta_2 \prod_{i < j} \left| 2 \sin \left( \frac{\theta_i - \theta_j}{2} \right) \right|^2. \tag{19}
\end{aligned}$$

The VanderMonde potential is stemmed from the invariance Haar measure of the group integration and is defined by

$$\mathcal{V}_{VdM}(\mathbf{g}) = -\frac{1}{\beta} G_{sym} \sum_{i < j}^{N_c} \log_e \left[ 2 \sin \left( \frac{\theta_i - \theta_j}{2} \right) \right], \tag{20}$$

where the parameter  $G_{sym}$  depends basically on the group's symmetry. It is reduced to  $G_{sym} = 2$  for  $SU(N_c)$ . In the lattice modeling, the number of states for the VanderMonde potential [2] [33] is introduced by  $\int d^d x \delta^d(0)$  as follows

$$\begin{aligned}
\sum (\text{states}) &\rightarrow \frac{1}{a^3} \int dV, \\
&\rightarrow \frac{V}{a^3}, \tag{21}
\end{aligned}$$

where  $a^3$  is the lattice size. Hence, the VanderMonde potential is regulated [2] as follows

$$\mathcal{V}_{VdM}(\mathbf{g}) = -\frac{1}{\beta} G_{sym} \left( \frac{V}{a^3} \right) \sum_{i < j}^{N_c} \log_e \left[ 2 \sin \left( \frac{\theta_i - \theta_j}{2} \right) \right]. \tag{22}$$

A finite bag with volume at the same size order of the lattice  $V \sim a^3 \sim \text{fm}^3$  and  $\frac{1}{a^3}V \sim 1$  is considered in the present work. The regulation  $\gamma_{reg} = \frac{V}{a^3}$  will be considered elsewhere. However, the term  $\frac{1}{a^3}V$  in MIT bag model is related to the volume fluctuation for a bag with an extended surface. Nonetheless, the VanderMonde potential regulation is essential for a



system with infinite volume [2]. Hereinafter, the number of states is considered  $\frac{1}{a^3}V \equiv 1$  for VanderMonde potential in colorless quark and gluon bag.

In order to consider Polyakov loops parameterization, it is useful to perform the variable transformation from fundamental gauge fields, namely,  $(\theta_1, \theta_2, \theta_3)$  with  $\theta_3 = -\theta_1 - \theta_2$  to Polyakov loop variables, namely,  $(\Phi, \bar{\Phi})$ . In the context of  $SU(3)_c$ , the invariance Haar measure is furnished by

$$\begin{aligned} \int d\mu(\mathbf{g}) &= \frac{1}{N!} \frac{1}{(2\pi)^2} \int_{-\pi}^{\pi} d\theta_1 \int_{-\pi}^{\pi} d\theta_2 \prod_{i < j} \left| 2 \sin \left( \frac{\theta_i - \theta_j}{2} \right) \right|^2, \\ &= \frac{1}{N!} \frac{1}{(2\pi)^2} \int_{-\pi}^{\pi} d\theta_1 \int_{-\pi}^{\pi} d\theta_2 \left( 27 \left[ 1 - 6\Phi\bar{\Phi} + 4 \left( \Phi^3 + \bar{\Phi}^3 \right) - 3 (\Phi\bar{\Phi})^2 \right] \right). \end{aligned} \quad (23)$$

The invariance Haar measure can be transformed and written in the terms of Polyakov loop variables  $\Phi$  and  $\bar{\Phi}$ . The transformation of the square root of the invariance Haar measure from the variable set  $\{\theta_i\}$  to  $\Phi$  and  $\bar{\Phi}$  leads to

$$\prod_{i < j} \left| 2 \sin \left( \frac{\theta_i - \theta_j}{2} \right) \right| = \left( 27 \left[ 1 - 6\Phi\bar{\Phi} + 4 \left( \Phi^3 + \bar{\Phi}^3 \right) - 3 (\Phi\bar{\Phi})^2 \right] \right)^{\frac{1}{2}}. \quad (24)$$

The integration over  $\theta_1$  and  $\theta_2$  is transformed to Polyakov loop variables  $\Phi$  and  $\bar{\Phi}$  as follows

$$\begin{aligned} \int d\theta_1 d\theta_2 &= \int d\Phi d\bar{\Phi} \left| \frac{\partial(\Phi, \bar{\Phi})}{\partial(\theta_1, \theta_2)} \right|^{-1}, \\ &= \int d\Phi d\bar{\Phi} \left( 27 \left[ 1 - 6\Phi\bar{\Phi} + 4 \left( \Phi^3 + \bar{\Phi}^3 \right) - 3 (\Phi\bar{\Phi})^2 \right] \right)^{-\frac{1}{2}}. \end{aligned} \quad (25)$$

Hence, the invariance Haar measure that is given by Eq.(19) becomes

$$\int d\mu(\mathbf{g}) = N_{\text{Haar}} \int_C d\Phi \int_C d\bar{\Phi} \left[ 1 - 6\Phi\bar{\Phi} + 4 \left( \Phi^3 + \bar{\Phi}^3 \right) - 3 (\Phi\bar{\Phi})^2 \right]^{\frac{1}{2}}, \quad (26)$$

where  $N_{\text{Haar}} = \frac{\sqrt{27}}{N_c! (2\pi)^{N_c-1}}$  for  $SU(3)_c$ . The subscript notation, namely,  $C$  that appears under the integral indicates the integration is over a complex plane domain. The complex domain for  $\Phi$  and  $\bar{\Phi}$  is the three pointed star with a radius 1. The complex domain for Polyakov loops complicates the situation when the non-Gaussian stationary point method fails and the Gaussian saddle point procedure turns to be essential. The invariance Haar measure with Polyakov loops parameterization can be represented as an effective Polyakov VanderMonde (PVdM) potential. The colorless canonical ensemble with an effective PVdM

potential in  $SU(3)_c$  group representation reads

$$\begin{aligned}
Z_{colorless}(\beta, V) &= N_{\text{Haar}} \int_C d\Phi \int_C d\bar{\Phi} \left[ 1 - 6\Phi\bar{\Phi} + 4(\Phi^3 + \bar{\Phi}^3) - 3(\Phi\bar{\Phi})^2 \right]^{\frac{1}{2}} \\
&\quad \times Z_{q\bar{q}g}(\beta, V; \Phi, \bar{\Phi}), \\
&= N_{\text{Haar}} \int_C d\Phi \int_C d\bar{\Phi} e^{-\beta[\mathcal{V}_{PVdM}(\beta; \Phi, \bar{\Phi}) + \Omega_{q\bar{q}g}(\beta, V; \Phi, \bar{\Phi})]},
\end{aligned} \tag{27}$$

where PVdM potential in  $SU(3)_c$  representation is given by

$$\mathcal{V}_{PVdM}(\beta; \Phi, \bar{\Phi}) = -\frac{1}{2} \frac{1}{\beta} \log_e \left( 1 - 6\Phi\bar{\Phi} + 4(\Phi^3 + \bar{\Phi}^3) - 3(\Phi\bar{\Phi})^2 \right), \tag{28}$$

and

$$\Omega_{q\bar{q}g}(\beta, V; \Phi, \bar{\Phi}) = -\frac{1}{\beta} \log_e [Z_{q\bar{q}g}(\beta, V; \Phi, \bar{\Phi})]. \tag{29}$$

The phenomenological PVdM potential can be introduced by adding a phenomenological pre-factor parameter, namely,  $\alpha_{ph}$ , in front of the logarithm as follows

$$\mathcal{V}_{PVdM}(\beta; \Phi, \bar{\Phi}) = -\frac{1}{2} \frac{1}{\beta} \alpha_{ph} \log_e \left( 1 - 6\Phi\bar{\Phi} + 4(\Phi^3 + \bar{\Phi}^3) - 3(\Phi\bar{\Phi})^2 \right). \tag{30}$$

This phenomenological parameter, namely,  $\alpha_{ph}$  modifies the underlying internal symmetry of Hagedorn states and in some scenarios this could break the internal symmetry of the QG-bags but not the global symmetry of the system [14]. The phenomenological PVdM potential and the variation of the phenomenological parameter,  $\alpha_{ph}$ , will be considered in another work. The integral that is given by Eq.(27) is evaluated using the non-Gaussian stationary points method over the complex plane. The Polyakov's stationary points, namely,  $\Phi = \Phi_0$  and  $\bar{\Phi} = \bar{\Phi}_0$  are evaluated by extremizing the exponent term. The stationary points  $\Phi_0$  and  $\bar{\Phi}_0$  are calculated as follows

$$\begin{aligned}
\frac{1}{V} \frac{\partial}{\partial \Phi} [\mathcal{V}_{PVdM}(\beta; \Phi, \bar{\Phi}) + \Omega_{q\bar{q}g}(\beta, V; \Phi, \bar{\Phi})] \Big|_{\Phi=\Phi_0, \bar{\Phi}=\bar{\Phi}_0} &= 0, \\
\frac{1}{V} \frac{\partial}{\partial \bar{\Phi}} [\mathcal{V}_{PVdM}(\beta; \Phi, \bar{\Phi}) + \Omega_{q\bar{q}g}(\beta, V; \Phi, \bar{\Phi})] \Big|_{\Phi=\Phi_0, \bar{\Phi}=\bar{\Phi}_0} &= 0.
\end{aligned} \tag{31}$$

The  $\Phi$ 's extremum is determined by the following constraint,

$$\begin{aligned}
\frac{3}{V} \frac{[\bar{\Phi} - 2\Phi^2 + \Phi\bar{\Phi}^2]}{[1 - 6\Phi\bar{\Phi} + 4(\Phi^3 + \bar{\Phi}^3) - 3(\Phi\bar{\Phi})^2]} &= \\
2 \sum_q^{N_f} \int \frac{p^2 dp}{2\pi^2} \frac{3e^{-\beta(\epsilon_q(\vec{p}) - \mu_q)}}{[1 + 3(\Phi + \bar{\Phi}e^{-\beta(\epsilon_q(\vec{p}) - \mu_q)})e^{-\beta(\epsilon_q(\vec{p}) - \mu_q)} + e^{-3\beta(\epsilon_q(\vec{p}) - \mu_q)}]} & \\
+ 2 \sum_q^{N_f} \int \frac{p^2 dp}{2\pi^2} \frac{3e^{-2\beta(\epsilon_q(\vec{p}) + \mu_q)}}{[1 + 3(\bar{\Phi} + \Phi e^{-\beta(\epsilon_q(\vec{p}) + \mu_q)})e^{-\beta(\epsilon_q(\vec{p}) + \mu_q)} + e^{-3\beta(\epsilon_q(\vec{p}) + \mu_q)}]} & + \omega_g T^3 \bar{\Phi}.
\end{aligned} \tag{32}$$

The same thing can be done for  $\overline{\Phi}$ . As far as the nuclear matter environment remains in the circumstance that Polyakov's stationary points are located in the region  $\Phi_0 < 1$  and  $\overline{\Phi}_0 < 1$  (i.e. non-Gaussian stationary points) and below the threshold of GW-like phase transition, then the canonical ensemble which is given by Eq.(27), is evaluated as follows

$$Z_{colorless}^{(I)}(\beta, V) = \exp \left( -\beta \left[ \mathcal{V}_{PVdM}(\beta; \Phi_0, \overline{\Phi}_0) + \Omega_{q\bar{q}g}(\beta, V; \Phi_0, \overline{\Phi}_0) \right] \right). \quad (33)$$

The pre-factor constant, namely  $N_{\text{Haar}}$ , that appears in Eq.(27) is dropped in order to normalize the partition function. The solution that is given by Eq.(33) is assigned as the low-lying energy solution (I). This solution is the asymptotic solution below the threshold of GW-like phase transition point. The validity of the low-lying energy solution (I) is satisfied as far Polyakov's non-Gaussian stationary points remain in the energy domain  $\Phi_0 \ll 1$  and  $\overline{\Phi}_0 \ll 1$  (i.e. far away from Polyakov triality restoration point). In the case that  $\mu_q = 0$ , then the equations' set given by Eq.(32) becomes symmetry over Polyakov loop variables and this leads to equal and real stationary points for  $\Phi$  and  $\overline{\Phi}$ . However, whenever  $|\Phi|_0 \rightarrow 1^-$ , then the effective PVdM potential, namely  $\mathcal{V}_{PVdM}(\beta; \Phi, \overline{\Phi})$ , develops a virtual logarithmic divergence. Therefore, the logarithmic divergence of the effective PVdM potential spoils badly Polyakov's non-Gaussian stationary points procedure and leads to virtual singularity for the effective grand potential of the system. Evidently, this virtual singularity deforms the low-lying energy solution  $Z_{colorless}^{(I)}(\beta, V)$ . This kind of behavior indicates modification in the analytic behavior of the canonical ensemble and another analytical solution, namely the solution (II) emerges in the system. The change in the analytical solution is the beneath mechanism of GW-like phase transition even for finite number of colors (i.e.  $N_c = 3$ ). The GW-like point for  $N_c = 3$  may play a significant role in the deconfinement phase transition diagram in nuclear physics as far it is not a confinement/deconfinement point. At the onset of GW-like phase transition, the non-Gaussian stationary points turn to behave as Gaussian saddle points that oscillate harmonically around the stationary points. This mechanism reflects the modification in the analytical behavior from the asymptotic solution (I) to the solution (II) when the temperature reaches GW-like point. Therefore, when GW-like threshold is reached, the canonical ensemble modifies its characteristic behavior from the low-lying energy solution  $Z_{colorless}^{(I)}(\beta, V)$  to the high-lying energy solution  $Z_{colorless}^{(II)}(\beta, V)$ . The second solution implies a possible production of Hagedorn states. When the asymptotic high-lying energy solution ( i.e. solution (II) ) is reached, it becomes more suitable to

write the invariance Haar measure in the terms of fundamental gauge fields (i.e.  $\theta_1, \theta_2, \theta_3 = -\theta_1 - \theta_2$ ) rather than Polyakov loop variables (i.e.  $\Phi, \bar{\Phi}$ ). Therefore, at the threshold of GW-like phase transition, the colorless canonical ensemble ( i.e. solution (II) ) is reduced to

$$Z_{colorless}^{(II)}(\beta, V) = Z_{q\bar{q}g}^{(0)}(\beta, V) \times \frac{1}{(2\pi)^2} \frac{1}{N!} \int_{-\infty}^{\infty} d\theta_1 \int_{-\infty}^{\infty} d\theta_2 \prod_{i < j} |\theta_i - \theta_j|^2 \times \exp \left[ -\frac{1}{2} a_{11}(\beta, V) \theta_1^2 - a_{12}(\beta, V) \theta_1 \theta_2 - \frac{1}{2} a_{22}(\beta, V) \theta_2^2 \right], \quad (34)$$

where

$$Z_{q\bar{q}g}^{(0)}(\beta, V) = Z_{q\bar{q}g}(\beta, V; \theta_1, \theta_2) \Big|_{\theta_1=0, \theta_2=0}, \quad (35)$$

and

$$\begin{aligned} a_{11}(\beta, V) &= \frac{\partial^2}{\partial \theta_1^2} \log_e Z_{q\bar{q}g}(\beta, V; \theta_1, \theta_2) \Big|_{\theta_1=0, \theta_2=0}, \\ a_{12}(\beta, V) &= \frac{\partial^2}{\partial \theta_1 \partial \theta_2} \log_e Z_{q\bar{q}g}(\beta, V; \theta_1, \theta_2) \Big|_{\theta_1=0, \theta_2=0}, \\ a_{22}(\beta, V) &= \frac{\partial^2}{\partial \theta_2^2} \log_e Z_{q\bar{q}g}(\beta, V; \theta_1, \theta_2) \Big|_{\theta_1=0, \theta_2=0}. \end{aligned} \quad (36)$$

Furthermore, in the case of massless flavors and zero flavor chemical potential (i.e.  $\mu_q = 0$ ), the canonical ensemble (II) for the high lying energy solution is simplified to

$$Z_{colorless}^{(II)}(\beta, V) = \frac{\left( \prod_{n=1}^{N_c-1} n! \right) \exp \left[ \frac{V}{\beta^3} \left( \frac{\pi^2}{45} (N_c^2 - 1) + \frac{7\pi^2}{180} N_c N_f + \frac{1}{4\pi^2} N_c N_f \Lambda^4 \beta^4 \right) \right]}{\sqrt{N_c} (2\pi)^{\frac{N_c-1}{2}} \left[ \frac{V}{\beta^3} \left( \frac{1}{3} N_f + \frac{2\pi^2}{45} \frac{N_c^2-1}{N_c} \right) \right]^{\frac{N_c^2}{2}-\frac{1}{2}}} \quad (37)$$

In the present model, the order parameter(s) of GW-like phase transition is (are) temperature (and/or flavor chemical potentials). At that critical point  $T = T_c$ , the low-lying and high-lying energy solutions match each other. In this case, the low-lying energy solution is extrapolated to the high-lying energy solution at the threshold of GW-like point. The critical value of  $T_c = 1/\beta_c$  is determined by the continuity condition

$$Z_{colorless}^{(I)}(\beta, V) \Big|_{\beta=\beta_c} = Z_{colorless}^{(II)}(\beta, V) \Big|_{\beta=\beta_c}. \quad (38)$$

Below GW-like point, the non-Gaussian stationary point of the asymptotic solution (I) is limited to  $|\Phi| < 1$ . At the threshold of GW-like phase transition, the non-Gaussian stationary points turn to be Gaussian saddle points that oscillate in the neighborhood of the center

of the symmetry group. Hence, the solution (II) turns to the asymptotic solution above GW-like point. The exact solution of Eq.(18) is obtained by evaluating the integration over the invariance Haar measure numerically. It is found that the asymptotic solution (I) matches the exact numerical solution below GW-like point while the solution (II) matches the exact one above GW-like point. Solutions (I) and (II) intersect each other in the neighborhood of GW-like point. The Gaussian saddle points procedure is better understood in the terms of fundamental gauge field variables  $\theta_i$  rather than Polyakov loop variables  $\Phi$  and  $\bar{\Phi}$ . Furthermore, the deconfinement phase transition takes place when the high-lying energy states of quark-gluon bags become unstable and in this case the Hagedorn matter undergoes phase transition to quark-gluon plasma at Hagedorn's temperature. It is worth to note here that below Hagedorn's temperature, the high-lying energy quark-gluon bag acts as quark-gluon fluid (or semi-QGP) droplets as far the constituent quarks and gluons remain within the range of the effective VanderMonde potential interaction.

### III. THE EXTENSION TO POLYAKOV-NAMBU-JONA-LASINIO MODEL

The conventional NJL Lagrangian density reads

$$\mathcal{L}_{NJL} = \bar{q} [i\gamma^\mu \partial_\mu - m_q] q + \frac{1}{2} G [(\bar{q}q)^2 + (\bar{q}i\gamma_5 \vec{\tau} q)^2], \quad (39)$$

where  $m_q$  is the quark's current mass and  $G$  is the NJL coupling constant. The constant  $G$  is adjusted in order to fit the nuclear phenomenology. The current mass and coupling constant for light flavors are taken  $m_q = 5$  MeV and  $G = 10.992$ , respectively. The quark and antiquark grand potential density in the presence of the effective chiral field is furnished by

$$\begin{aligned} \frac{\Omega_{q\bar{q}}(\beta, V; \sigma, \Phi, \bar{\Phi})}{V} = & -2N_c \sum_q^{N_f} \int \frac{d^3\vec{p}}{(2\pi)^3} E_{q\sigma}(\vec{p}) - \frac{1}{\pi^2} \sum_q^{N_f} \int d|\vec{p}| \frac{|\vec{p}|^4}{E_{q\sigma}(\vec{p})} \\ & \times \left( \frac{[(\Phi + 2\bar{\Phi}e^{-\beta[E_{q\sigma}(\vec{p})-\mu_q]})e^{-\beta[E_{q\sigma}(\vec{p})-\mu_q]} + e^{-3\beta[E_{q\sigma}(\vec{p})-\mu_q]}]}{[1 + 3(\Phi + \bar{\Phi}e^{-\beta[E_{q\sigma}(\vec{p})-\mu_q]})e^{-\beta[E_{q\sigma}(\vec{p})-\mu_q]} + e^{-3\beta[E_{q\sigma}(\vec{p})-\mu_q]}]} \right. \\ & \left. + \frac{[(\bar{\Phi} + 2\Phi e^{-\beta[E_{q\sigma}(\vec{p})+\mu_q]})e^{-\beta[E_{q\sigma}(\vec{p})+\mu_q]} + e^{-3\beta[E_{q\sigma}(\vec{p})+\mu_q]}]}{[1 + 3(\bar{\Phi} + \Phi e^{-\beta[E_{q\sigma}(\vec{p})+\mu_q]})e^{-\beta[E_{q\sigma}(\vec{p})+\mu_q]} + e^{-3\beta[E_{q\sigma}(\vec{p})+\mu_q]}]} \right) \quad (40) \end{aligned}$$

where  $E_{q\sigma}(\vec{p}) = \sqrt{\vec{p}^2 + M_q(\sigma)^2}$  and  $M_q(\sigma) = m_q - G\sigma$ . The parameters  $m_q$ ,  $\sigma$ ,  $\Phi$ ,  $G$  and  $\mu_q$  are quark's current mass, scalar field, Polyakov loop parameter, scalar coupling constant

and constituent quark's chemical potential, respectively. The  $\sigma$  scalar mean field indicates the condensate  $\sigma = \langle q\bar{q} \rangle$ . The first term on the right hand side of Eq.(40) is temperature independent and is regularized as follows,

$$\int_0^\Lambda \frac{d^3\vec{p}}{(2\pi)^3} E_{q\sigma}(\vec{p}) = \frac{1}{2\pi^2} \left[ \frac{1}{8} m_q(\sigma)^2 \Lambda \sqrt{m_q(\sigma)^2 + \Lambda^2} + \frac{1}{4} \Lambda^3 \sqrt{m_q(\sigma)^2 + \Lambda^2} - \frac{1}{8} m_q(\sigma)^4 \log_e \left( \sqrt{1 + \frac{\Lambda^2}{m_q(\sigma)^2}} + \frac{\Lambda}{|m_q(\sigma)|} \right) \right], \quad (41)$$

where the UV-cutoff  $\Lambda = 631.5$  MeV. The scalar  $\sigma$ -chiral field in the context of PNJL model is considered self-consistently. In the terms of fundamental gauge fields  $(\theta_1, \theta_2, \theta_3 = -\theta_1 - \theta_2)$  rather than Polyakov loops  $(\Phi, \bar{\Phi})$ , Eq.(40) is reduced to

$$-\frac{\Omega_{q\bar{q}}(\beta, V; \sigma, \Phi, \bar{\Phi})}{V} = -\frac{\Omega_{q\bar{q}}(\beta, V; \sigma, \Phi(\theta_1, \theta_2), \bar{\Phi}(\theta_1, \theta_2))}{V}, \\ \rightarrow -\frac{\Omega_{q\bar{q}}(\beta, V; \sigma, \theta_1, \theta_2)}{V}, \quad (42)$$

where

$$-\frac{\Omega_{q\bar{q}}(\beta, V; \sigma, \theta_1, \theta_2)}{V} = 2N_c \sum_q \int_0^\Lambda \frac{d|\vec{p}| |\vec{p}|^2}{2\pi^2} E_{q\sigma}(\vec{p}) \\ + 2 \sum_q \sum_{k=1}^{N_c} \int \frac{d|\vec{p}|}{(2\pi^2)} \frac{|\vec{p}|^4}{3E_{q\sigma}(\vec{p})} \left( \frac{1 + \cos(\theta_k) e^{\beta[E_{q\sigma}(\vec{p}) - \mu_q]}}{1 + 2 \cos(\theta_k) e^{\beta[E_{q\sigma}(\vec{p}) - \mu_q]} + e^{2\beta[E_{q\sigma}(\vec{p}) - \mu_q]}} \right. \\ \left. + \frac{1 + \cos(\theta_k) e^{\beta[E_{q\sigma}(\vec{p}) + \mu_q]}}{1 + 2 \cos(\theta_k) e^{\beta[E_{q\sigma}(\vec{p}) + \mu_q]} + e^{2\beta[E_{q\sigma}(\vec{p}) + \mu_q]}} \right) \\ + i 2 \sum_q \sum_{k=1}^{N_c} \int \frac{d|\vec{p}|}{(2\pi^2)} \frac{|\vec{p}|^4}{3E_{q\sigma}(\vec{p})} \left( \frac{e^{\beta[E_{q\sigma}(\vec{p}) - \mu_q]} \sin(\theta_k)}{1 + 2 \cos(\theta_k) e^{\beta[E_{q\sigma}(\vec{p}) - \mu_q]} + e^{2\beta[E_{q\sigma}(\vec{p}) - \mu_q]}} \right. \\ \left. - \frac{e^{\beta[E_{q\sigma}(\vec{p}) + \mu_q]} \sin(\theta_k)}{1 + 2 \cos(\theta_k) e^{\beta[E_{q\sigma}(\vec{p}) + \mu_q]} + e^{2\beta[E_{q\sigma}(\vec{p}) + \mu_q]}} \right). \quad (43)$$

Therefore, in the case  $\mu_q = 0$ , Eq.(43) becomes real and is simplified to

$$-\frac{\Omega_{q\bar{q}}(\beta, V; \sigma, \theta_1, \theta_2)}{V} = 2N_c \sum_q \int_0^\Lambda \frac{d|\vec{p}| |\vec{p}|^2}{2\pi^2} E_{q\sigma}(\vec{p}) \\ + 4 \sum_q \sum_{k=1}^{N_c} \int \frac{d|\vec{p}|}{(2\pi^2)} \frac{|\vec{p}|^4}{3E_{q\sigma}(\vec{p})} \left( \frac{1 + \cos(\theta_k) e^{\beta E_{q\sigma}(\vec{p})}}{1 + 2 \cos(\theta_k) e^{\beta E_{q\sigma}(\vec{p})} + e^{2\beta E_{q\sigma}(\vec{p})}} \right). \quad (44)$$

Subsequently, the canonical ensemble for quarks and gluons in the context of the PNJL model becomes

$$Z_{q\bar{q}g}(\beta, V; \sigma, \Phi, \bar{\Phi}) = \exp[-\beta \Omega_{q\bar{q}g}(\beta, V; \sigma, \Phi, \bar{\Phi})]. \quad (45)$$

The total grand potential for chiral quarks and gluons reads

$$\Re \Omega_{q\bar{q}g}(\beta, V; \sigma, \Phi, \bar{\Phi}) = \Omega_{q\bar{q}}(\beta, \sigma; \Phi, \bar{\Phi}) + \Omega_g(\beta, V; \Phi, \bar{\Phi}) + V U(\sigma), \quad (46)$$

where  $V$  is the system's volume. The chiral quark and antiquark grand potential  $\Omega_{q\bar{q}}(\beta, V; \sigma, \Phi, \bar{\Phi})$  is determined by Eq.(40) while the gluon grand potential  $\Omega_g(\beta, V; \Phi, \bar{\Phi})$  is determined from Eq.(13). The effective chiral potential is given by

$$U(\sigma) = \frac{1}{2} G \sigma^2. \quad (47)$$

The canonical ensemble for the colorless quark and gluon blob is determined by projecting the color-singlet state in the following way,

$$\begin{aligned} Z_{colorless}(\beta, V; \sigma) &= \int d\mu(\mathbf{g}) Z_{q\bar{q}g}(\beta, V; \sigma, \Phi, \bar{\Phi}), \\ &= \int d\mu(\mathbf{g}) Z_{q\bar{q}g}(\beta, V; \sigma, \theta_1, \theta_2). \end{aligned} \quad (48)$$

It is possible to write Eq.(48) in the terms of Polyakov loop variables  $\Phi$  and  $\bar{\Phi}$  as follows

$$Z_{colorless}(\beta, V; \sigma) = N_{\text{Haar}} \int_C d\Phi \int_C d\bar{\Phi} Z_{PNJL}(\beta, V; \sigma, \Phi, \bar{\Phi}), \quad (49)$$

where the subscript  $C$  indicates the integration over the three pointed star boundary in the complex plane and

$$Z_{PNJL}(\beta, V; \sigma, \Phi, \bar{\Phi}) = \exp(-\beta [\mathcal{V}_{PVD}(\beta; \Phi, \bar{\Phi}) + \Omega_{q\bar{q}g}(\beta, V; \sigma, \Phi, \bar{\Phi})]). \quad (50)$$

The double integrations over Polyakov loop variables, namely,  $\Phi, \bar{\Phi}$  is evaluated using the non-Gaussian stationary points method for the low-lying energy limit. Subsequently using the non-Gaussian stationary points method, Eq.(49) is reduced to the low-lying energy solution as follows,

$$\begin{aligned} Z_{colorless}^{(I)}(\beta, V; \sigma) &= Z_{colorless}^{(I)}(\beta, V; \sigma, \Phi_0, \bar{\Phi}_0), \\ &= Z_{PNJL}(\beta, V; \sigma, \Phi_0, \bar{\Phi}_0), \\ &= \exp(-\beta [\mathcal{V}_{PVD}(\beta; \Phi_0, \bar{\Phi}_0) + \Omega_{q\bar{q}g}(\beta, V; \sigma, \Phi_0, \bar{\Phi}_0)]). \end{aligned} \quad (51)$$

The pre-factor  $N_{\text{Haar}}$  is eliminated in order to guarantee the normalization of the non-Gaussian stationary point method and it does not affect the calculation. The Polyakov loops' non-Gaussian stationary points, namely,  $\Phi_0$  and  $\bar{\Phi}_0$  are determined by extremizing

the exponent which appears on the right hand side of Eq.(50) with respect to  $\Phi$  and  $\bar{\Phi}$  in the following way,

$$\begin{aligned} \frac{\partial}{\partial \Phi} [\mathcal{V}_{PVdM}(\beta; \Phi, \bar{\Phi}) + \Omega_{q\bar{q}g}(\beta, V; \sigma, \Phi, \bar{\Phi})] \Big|_{\Phi=\Phi_0, \bar{\Phi}=\bar{\Phi}_0} &= 0, \\ \frac{\partial}{\partial \bar{\Phi}} [\mathcal{V}_{PVdM}(\beta; \Phi, \bar{\Phi}) + \Omega_{q\bar{q}g}(\beta, V; \sigma, \Phi, \bar{\Phi})] \Big|_{\Phi=\Phi_0, \bar{\Phi}=\bar{\Phi}_0} &= 0. \end{aligned} \quad (52)$$

Furthermore, the  $\sigma$ -chiral field stationary point, namely  $\sigma_0$ , is determined by extremizing the exponent which appears on the right hand side of Eq.(51) with respect to the scalar field  $\sigma$ . Since Polyakov VanderMonde potential, namely,  $\mathcal{V}_{PVdM}(\beta; \Phi, \bar{\Phi})$  does not depend on  $\sigma$ , the variation of  $\Omega_{q\bar{q}g}(\beta, V; \sigma, \Phi_0, \bar{\Phi}_0)$  with respect to  $\sigma$  mean field leads to

$$\sigma = -\frac{1}{G} \frac{\partial}{\partial \sigma} \left( \frac{\Omega_{q\bar{q}}(\beta, V; \sigma, \Phi_0, \bar{\Phi}_0)}{V} \right) \Big|_{\sigma=\sigma_0}, \quad (53)$$

where

$$\begin{aligned} -\frac{\partial}{\partial \sigma} \left( \frac{\Omega_{q\bar{q}}(\beta, V; \sigma, \Phi, \bar{\Phi})}{V} \right) &= \sum_q^{N_f} \left( M_q(\sigma) \frac{\partial}{\partial \sigma} M_q(\sigma) \right) \left[ 2N_c \int_0^\Lambda \frac{d|\vec{p}|}{2\pi^2} \frac{|\vec{p}|^2}{E_{q\sigma}(\vec{p})} \right. \\ &\quad - 6 \int_0^\infty \frac{d|\vec{p}|}{2\pi^2} \frac{|\vec{p}|^2}{E_{q\sigma}(\vec{p})} \frac{(\Phi + 2\bar{\Phi}e^{-\beta E_{q\sigma}(\vec{p})}) e^{-\beta E_{q\sigma}(\vec{p})} + e^{-3\beta E_{q\sigma}(\vec{p})}}{[1 + 3(\Phi + \bar{\Phi}e^{-\beta E_{q\sigma}(\vec{p})}) e^{-\beta E_{q\sigma}(\vec{p})} + e^{-3\beta E_{q\sigma}(\vec{p})}]} \\ &\quad \left. - 6 \int_0^\infty \frac{d|\vec{p}|}{2\pi^2} \frac{|\vec{p}|^2}{E_{q\sigma}(\vec{p})} \frac{(\bar{\Phi} + 2\Phi e^{-\beta E_{q\sigma}(\vec{p})}) e^{-\beta E_{q\sigma}(\vec{p})} + e^{-3\beta E_{q\sigma}(\vec{p})}}{[1 + 3(\bar{\Phi} + \Phi e^{-\beta E_{q\sigma}(\vec{p})}) e^{-\beta E_{q\sigma}(\vec{p})} + e^{-3\beta E_{q\sigma}(\vec{p})}]} \right] \end{aligned} \quad (54)$$

Moreover, when Eq.(54) is written in the terms of fundamental gauge fields  $(\theta_1, \theta_2)$ , it is reduced to

$$\begin{aligned} -\frac{\partial}{\partial \sigma} \left( \frac{\Omega_{q\bar{q}}(\beta, V; \sigma, \theta_1, \theta_2)}{V} \right) &= \sum_q^{N_f} \left( M_q(\sigma) \frac{\partial}{\partial \sigma} M_q(\sigma) \right) \left[ 2N_c \int_0^\Lambda \frac{d|\vec{p}|}{2\pi^2} \frac{|\vec{p}|^2}{E_{q\sigma}(\vec{p})} \right. \\ &\quad \left. - 4 \sum_{k=1}^{N_c} \int_0^\infty \frac{d|\vec{p}|}{2\pi^2} \frac{|\vec{p}|^2}{E_{q\sigma}(\vec{p})} \frac{1 + e^{\beta E_{q\sigma}(\vec{p})} \cos(\theta_k)}{1 + 2e^{\beta E_{q\sigma}(\vec{p})} \cos(\theta_k) + e^{2\beta E_{q\sigma}(\vec{p})}} \right]. \end{aligned} \quad (55)$$

The first term inside the square bracket on the right hand side of Eq.(54) and/or Eq.(55) is temperature independent. Its explicit expression reads

$$\begin{aligned} \int_0^\Lambda \frac{d|\vec{p}|}{2\pi^2} \frac{|\vec{p}|^2}{E_{q\sigma}(\vec{p})} &= \frac{1}{4\pi^2} \Lambda \sqrt{M_q(\sigma)^2 + \Lambda^2} \\ &\quad - \frac{1}{4\pi^2} M_q(\sigma)^2 \log_e \left( \frac{\Lambda}{M_q(\sigma)} + \sqrt{1 + \left( \frac{\Lambda}{M_q(\sigma)} \right)^2} \right). \end{aligned} \quad (56)$$



Therefore, the partition function (i.e. the canonical ensemble) for the colorless quark and gluon bag with  $\sigma$ -chiral field reads

$$\begin{aligned}
Z_{colorless}^{(I)}(\beta, V) &= Z_{colorless}^{(I)}(\beta, V; \sigma_0), \\
&= Z_{colorless}^{(I)}(\beta, V; \sigma_0, \Phi_0, \bar{\Phi}_0), \\
&= Z_{PNJL}(\beta, V; \sigma_0, \Phi_0, \bar{\Phi}_0),
\end{aligned} \tag{57}$$

where the values of  $\Phi_0$ ,  $\bar{\Phi}_0$  and  $\sigma_0$  are the stationary points and they are calculated by Eqs.(52) and (53), respectively. Evidently, when the temperature approaches the critical one (i.e. GW-like point), the non-Gaussian stationary point method fails due to the logarithmic divergence of Polyakov VanderMonde potential, namely,  $\mathcal{V}_{PVM}(\beta; \Phi, \bar{\Phi})$ . The logarithmic divergence of Polyakov VanderMonde potential indicates a collapse of the non-Gaussian stationary point method for the low-lying energy solution and the emergence of the high-lying energy solution where Polyakov loops' stationary points switch to become Gaussian saddle points that oscillate harmonically around the non-Gaussian stationary points. The Gaussian saddle point procedure is understood in the context of fundamental gauge fields  $\theta_1$  and  $\theta_2$  much better than in the frame work of Polyakov loops  $\Phi$  and  $\bar{\Phi}$ .

On the other hand, the partition function for the asymptotic high-lying energy solution (i.e. solution II) for colorless quark and gluon blob in the context of PNJL model reads

$$\begin{aligned}
Z_{colorless}^{(II)}(\beta, V; \sigma) &= \int d\mu(\mathbf{g}) Z_{q\bar{q}g}(\beta, V; \sigma, \Phi, \bar{\Phi}), \\
&= \frac{1}{(2\pi)^2} \frac{1}{N!} \int_{-\infty}^{\infty} d\theta_1 \int_{-\infty}^{\infty} d\theta_2 \prod_{i < j} (\theta_i - \theta_j)^2 e^{-\beta \Omega_{q\bar{q}g}(\beta, V; \sigma, \theta_1, \theta_2)},
\end{aligned} \tag{58}$$

where  $\theta_3 = -\theta_1 - \theta_2$ . The quark and gluon grand potential which appears in the exponent in Eq.(58) is given by

$$\begin{aligned}
\Omega_{q\bar{q}g}(\beta, V; \sigma, \theta_1, \theta_2) &= \Omega_{q\bar{q}g}(\beta, V; \sigma, \Phi(\theta_1, \theta_2), \bar{\Phi}(\theta_1, \theta_2)), \\
&= \Omega_{q\bar{q}}(\beta, V; \sigma, \theta_1, \theta_2) + \Omega_g(\beta, V; \sigma, \theta_1, \theta_2) + V U(\sigma),
\end{aligned} \tag{59}$$

where  $V$  is the bag's volume and Polyakov loop parameters  $\Phi$  and  $\bar{\Phi}$  are written explicitly as functions of the fundamental gauge fields  $\theta_1$ ,  $\theta_2$  and  $\theta_3$ . The effective scalar potential, namely  $U(\sigma)$ , is given by Eq.(47). Since the non-Gaussian stationary points for the low-lying energy solution (I) are reduced to Gaussian saddle points for the asymptotic high-lying energy solution (II), it becomes essential to compute the quadratic expansion of the grand

potential around the Gaussian saddle points in order to evaluate the integral that is given in Eq.(58) more appropriately. This can be done much easier in the framework of fundamental gauge fields rather than Polyakov loops. The Gaussian saddle points of the fundamental gauge fields accumulate at the origin and fortunately this behavior simplifies the calculation drastically. The quadratic Taylor expansion of the grand potential density for quarks and anti-quarks is reduced to

$$\frac{1}{V}\Omega_{q\bar{q}}(\beta, V; \sigma, \theta_1, \theta_2) = \frac{1}{V}\Omega_{q\bar{q}}^{(0)}(\beta, V; \sigma) + \frac{1}{2}\frac{1}{V}\Omega_{q\bar{q}}^{(2)}(\beta, V; \sigma) \sum_i^{N_c} \theta_i^2, \quad (60)$$

where the 0<sup>th</sup> term reads

$$\begin{aligned} \frac{1}{V}\Omega_{q\bar{q}}^{(0)}(\beta, V; \sigma) = & -2N_c \sum_q^{N_f} \int_0^\Lambda \frac{d^3\vec{p}}{(2\pi)^3} E_{q\sigma}(\vec{p}) \\ & -4N_c \sum_q^{N_f} \int \frac{d|\vec{p}|}{2\pi^2} \frac{|\vec{p}|^4}{3E_{q\sigma}(\vec{p})} \frac{1}{[e^{\beta E_{q\sigma}(\vec{p})} + 1]}, \end{aligned} \quad (61)$$

while the quadratic term is given by

$$\frac{1}{V}\Omega_{q\bar{q}}^{(2)}(\beta, V; \sigma) = 4\frac{1}{\beta} \sum_q^{N_f} \int \frac{d|\vec{p}|}{2\pi^2} |\vec{p}|^2 \frac{e^{\beta E_{q\sigma}(\vec{p})}}{(e^{\beta E_{q\sigma}(\vec{p})} + 1)^2}. \quad (62)$$

Again, the gluonic grand potential for the low-lying energy colorless quark-gluon bags is assumed to be adjusted by the phenomenology as done in Sec.II (see for instance Eq.(13)). This class of the phenomenological gluon potential is inspired from lattice calculations and has been recently adopted widely in the literature (for instance see [4]). The quadratic Taylor expansion of the gluon grand potential which is given by Eq.(13) is approximated to

$$\frac{1}{V}\Omega_g(\beta, V) = \frac{1}{V}\Omega_g^{(0)}(\beta, V) + \frac{1}{2}\frac{1}{V}\Omega_g^{(2)}(\beta, V) \sum_{ij} (\theta_i - \theta_j)^2. \quad (63)$$

The 0<sup>th</sup> term reads

$$\frac{1}{V}\Omega_g^{(0)}(\beta, V) = -\frac{1}{\beta} \left( \frac{\omega_g}{\beta^3} \right), \quad (64)$$

while the quadratic term is reduced to

$$\frac{1}{V}\Omega_g^{(2)}(\beta, V) = \frac{1}{\beta} \frac{1}{N_c^2} \left( \frac{\omega_g}{\beta^3} \right), \quad (65)$$

where  $\omega_g = \frac{\pi^2(N_c^2-1)}{45}$ . After evaluating the Gaussian integration over the fundamental gauge fields, the partition function for the high-lying energy solution (i.e. solution II) is approximated to

$$Z_{colorless}^{(II)}(\beta, V) = Z_{colorless}^{(II)}(\beta, V; \sigma_0), \quad (66)$$

where

$$Z_{colorless}^{(II)}(\beta, V; \sigma) = \frac{\left(\prod_{n=1}^{N_c-1} n!\right) \exp\left(-\beta \left[\Omega_{q\bar{q}}^{(0)}(\beta, V; \sigma) + \Omega_g^{(0)}(\beta, V) + V U(\sigma)\right]\right)}{\sqrt{N_c}(2\pi)^{\frac{1}{2}(N_c-1)} \left(\beta \left[\Omega_{q\bar{q}}^{(2)}(\beta, V; \sigma) + 2N_c \Omega_g^{(2)}(\beta, V)\right]\right)^{\frac{N_c^2-1}{2}}} \quad (67)$$

Furthermore,  $\sigma$ -mean field (i.e.  $\sigma_0$ ), above the threshold of GW-like phase transition, is determined by calculating  $\sigma$ -stationary point in the following way,

$$\left. \frac{\partial}{\partial \sigma} \frac{\Omega_{q\bar{q}g}^{(II)*}(\beta, V; \sigma)}{V} \right|_{\sigma=\sigma_0} = 0, \quad (68)$$

where

$$\Omega_{q\bar{q}g}^{(II)*}(\beta, V; \sigma) = \Omega_{q\bar{q}}^{(0)}(\beta, V; \sigma) + \Omega_g^{(0)}(\beta, V) + V U(\sigma). \quad (69)$$

Under the assumption of the stationary point method, the extremization procedure is performed for the exponent term that appears in Eq.(67). The extremization of Eq.(68) leads to

$$G\sigma = -\frac{\partial}{\partial \sigma} \left( \frac{\Omega_{q\bar{q}}^{(0)}(\beta, V; \sigma)}{V} \right), \quad (70)$$

where

$$\begin{aligned} -\frac{\partial}{\partial \sigma} \left( \frac{\Omega_{q\bar{q}}^{(0)}(\beta, V; \sigma)}{V} \right) &= 2N_c \sum_q^{N_f} \left[ \int_0^\Lambda \frac{d|\vec{p}|}{2\pi^2} \frac{\vec{p}^2}{E_{q\sigma}(\vec{p})} - 2 \int \frac{d|\vec{p}|}{2\pi^2} \frac{\vec{p}^2}{E_{q\sigma}(\vec{p})} \frac{1}{(e^{\beta E_{q\sigma}(\vec{p})} + 1)} \right] \\ &\times \left( M_q(\sigma) \frac{\partial M_q(\sigma)}{\partial \sigma} \right). \end{aligned} \quad (71)$$

In order to calculate other thermodynamics quantities, the derivative of the partition function with respect to  $X$  is reduced to

$$\begin{aligned} -\frac{\partial}{\partial X} \frac{1}{\beta} \log_e \left[ Z_{colorless}^{(II)}(\beta, V; \sigma) \right] &= \frac{\partial}{\partial X} \Omega_{q\bar{q}}^{(0)}(\beta, V; \sigma) + \frac{\partial}{\partial X} \Omega_g^{(0)}(\beta, V) + \frac{\partial}{\partial X} [V U(\sigma)] \\ &+ \left( \alpha - \frac{1}{2} \right) \frac{\partial}{\partial X} \left\{ \frac{1}{\beta} \log_e \left( \beta \left[ \Omega_{q\bar{q}}^{(2)}(\beta, V; \sigma) + 2N_c \Omega_g^{(2)}(\beta, V) \right] \right) \right\}, \end{aligned} \quad (72)$$

where  $X$  is a thermodynamic ensemble such as  $\beta$  and  $V$ . For instance, from Eq.(72), the grand potential for colorless quark and gluon blob reads

$$\begin{aligned} \frac{1}{V} \Omega_{q\bar{q}g}^{(II)}(\beta, V; \sigma) &= -\frac{\partial}{\partial V} \frac{1}{\beta} \log_e \left[ Z_{colorless}^{(II)}(\beta, V; \sigma) \right], \\ &= \frac{\Omega_{q\bar{q}}^{(0)}(\beta, V; \sigma)}{V} + \frac{\Omega_g^{(0)}(\beta, V)}{V} + U(\sigma) - \frac{\alpha - \frac{1}{2}}{V}. \end{aligned} \quad (73)$$

Hence, if the  $\sigma$ -chiral field is not restored below GW-like point, then it will be a discontinuity (i.e. at least of a higher order discontinuity) from  $\sigma_0 = \sigma_0^{(I)}$  to  $\sigma_0 = \sigma_0^{(II)}$  in the neighborhood of GW-like point because the value of  $\sigma_0^{(I)}$  below GW-like point is determined by Eq.(53) while  $\sigma_0^{(II)}$  above GW-like point is determined by Eq.(68) or Eq.(70). However, the extensive numerical calculations show that the chiral symmetry restoration usually occurs in the neighborhood of GW-like point and before the ultimate point of the extended GW-range is reached. This indicates that the high-lying energy solution is chirally restored. It should be noted that in infinite volume limit, the VanderMonde regularization becomes essential and, subsequently, Eq.(67) is reduced to

$$Z_{colorless}^{(II)}(\beta, V) = Z_{colorless}^{(II)}(\beta, V; \sigma_0), \quad (74)$$

where

$$Z_{colorless}^{(II)}(\beta, V; \sigma) = \frac{\left( \prod_{n=1}^{N_c-1} n! \right)}{\sqrt{N_c} (2\pi)^{\frac{1}{2}(N_c-1)}} \frac{\exp \left( -\beta \Omega_{q\bar{q}g}^{(II)*}(\beta, V; \sigma) \right)}{\left( \beta \left[ \Omega_{q\bar{q}}^{(2)}(\beta, V; \sigma) + 2N_c \Omega_g^{(2)}(\beta, V) \right] \right)^{\gamma_{reg} \frac{(N_c^2-1)}{2}}}, \quad (75)$$

where  $\gamma_{reg} = \frac{V}{a^3}$  and  $a^3$  is the lattice space size. Nonetheless, the regularization procedure is not required for finite colorless quark and gluon bag.

The order parameter for GW-like phase transition is the temperature (and the chemical potentials). The point of the phase transition, namely,  $T_{GW}$  is determined by the continuity of the partition function from the low-lying energy solution to the high-lying one and this condition is satisfied when both solutions match each others as follows,

$$\begin{aligned} Z_{colorless}^{(I)}(\beta, V) &= Z_{colorless}^{(II)}(\beta, V) \Big|_{\beta=\beta_{GW}} \\ &\rightarrow Z_{colorless}^{(I)}(\beta_{GW}, V; \sigma^{(I)}) = Z_{colorless}^{(II)}(\beta_{GW}, V; \sigma^{(II)}). \end{aligned} \quad (76)$$

The values of  $\sigma^{(I)}$  and  $\sigma^{(II)}$  are determined using Eqs.(53) and (70), respectively. The both solutions (I) and (II) are asymptotic solutions for the low and high temperatures,

respectively. This implies that the solution (I)'s partition function is extrapolated to the solution (II) when the threshold of GW-like point is reached. Beyond that point, the solution (I) deviates significantly from the exact numerical one and turns to be no longer correct. Fortunately, the solution (II) provides a clue whereabouts GW-like point threshold and its ultimate point and also their interpolation range (i.e. the interval between the threshold and ultimate point). The Helmholtz free energy of solution (II) has a hidden valley. The validity of the asymptotic solution (II) is maintained whenever the energy climbs the hidden valley and reaches the same level of its virtual top that appears at lower temperature. This point is ultimate point of the extended interval of GW-like point. Beyond the ultimate point, solution (II) matches the exact one precisely. When solution (II) intersects solution (I), the threshold of an extended GW-like interval emerges. At GW-threshold, the solution (I) starts to deviate significantly and subsequently solution (II) turns to be the correct asymptotic solution instead of solution (I). The deviation becomes significant when GW-ultimate point is reached. Therefore, it is reasonable to interpolate solution (I) from GW-threshold to the asymptotic solution (II) at GW-ultimate point.

The PNJL-partition function can be solved exactly. The partition function for the colorless quark and gluon blob reads

$$Z_{colorless}(\beta, V) = Z_{colorless}(\beta, V; \sigma_0), \quad (77)$$

where

$$Z_{colorless}(\beta, V; \sigma) = \int_{-\pi}^{\pi} d\theta_1 \int_{-\pi}^{\pi} d\theta_2 \mu_{\text{Haar}}(\theta_1, \theta_2) \exp[-\beta \Omega_{q\bar{q}g}(\beta, V; \sigma, \theta_1, \theta_2)]. \quad (78)$$

The invariance Haar measure is given by

$$\mu_{\text{Haar}}(\theta_1, \theta_2) = \frac{\prod_{n=1}^{(N_c-1)} n!}{N_c! (2\pi)^{N_c-1}} \prod_{i < j} 4 \sin\left(\frac{\theta_i - \theta_j}{2}\right)^2. \quad (79)$$

Furthermore, chiral mean field, namely,  $\sigma_0$  is evaluated by extremizing the partition function as follows

$$-\frac{\partial}{\partial \sigma} \frac{1}{V\beta} \log_e [Z_{colorless}(\beta, V; \sigma)] \Big|_{\sigma=\sigma_0} = 0. \quad (80)$$

Thus Eq.(80) is reduced to

$$\begin{aligned} & \int_{-\pi}^{\pi} d\theta_1 \int_{-\pi}^{\pi} d\theta_2 \mu_{\text{Haar}}(\theta_1, \theta_2) \exp[-\beta \Omega_{q\bar{q}g}(\beta, V; \sigma, \theta_1, \theta_2)] \\ & \times \left[ \frac{\partial}{\partial \sigma} \frac{\Omega_{q\bar{q}g}(\beta, V; \sigma, \theta_1, \theta_2)}{V} \right] = 0. \end{aligned} \quad (81)$$

Hence by using Eqs.(80) and (81) the  $\sigma_0$ -chiral mean field is determined by solving the following equation,

$$\begin{aligned} \frac{\partial}{\partial \sigma} U(\sigma) = & \frac{1}{Z_{colorless}(\beta, V; \sigma)} \int_{-\pi}^{\pi} d\theta_1 \int_{-\pi}^{\pi} d\theta_2 \mu_{\text{Haar}}(\theta_1, \theta_2) \\ & \times \left[ -\frac{\partial}{\partial \sigma} \frac{\Omega_{q\bar{q}}(\beta, V; \sigma, \theta_1, \theta_2)}{V} \right] \exp[-\beta \Omega_{q\bar{q}g}(\beta, V; \sigma, \theta_1, \theta_2)]. \end{aligned} \quad (82)$$

#### IV. GW-LIKE POINT AND HAGEDORN STATES

The asymptotic mass spectral density of states is given by the micro-canonical ensemble. The micro-canonical ensemble can be derived from the mixed-grand canonical ensemble of a single QG-bag. It is given by the inverse Laplace transform as follows

$$\rho_{colorless}(W, V) \sim \frac{1}{2\pi i} \int_{\beta_0 - i\infty}^{\beta_0 + i\infty} d\beta e^{\beta W} Z_{colorless}(\beta, V), \quad (83)$$

where  $W$  is the energy of QG-bag. In the limit of large  $W$ , Eq.(83) is evaluated using the steepest descent method. The approximation of the steepest descent method fails in the limit of small  $W$ . This means that it is reasonable to replace the low-lying mass spectral density with the discrete mass spectrum of the hadron states while the high-lying mass spectral density in the large  $W$  limit is approximated to the bootstrap-like mass spectral density for Hagedorn states. Hence, it is more appropriate to replace solution (I) with the discrete mass spectrum of hadronic states. Furthermore, it will be shown below that the extrapolation of the mass spectral density of solution (I) to Hagedorn states does not lead to a deconfinement phase transition to QGP at Hagedorn's temperature. In contrary, the mass spectral density for solution (II) leads to a first order phase transition. Therefore, the existence of Hagedorn states is interpreted in the term of GW-like phase transition where the discrete hadronic mass spectrum turns to the continuous bootstrap-like mass spectrum when the hadron's mass exceeds a specific mass threshold (i.e.  $m_H > 2$  GeV). In order to simplify the calculation drastically, the chiral field is dropped in this section. The density

of states for solution (I) is reduced to

$$\begin{aligned}
\lim_{W \rightarrow \infty} \rho_{colorless}^{(I)}(W, V) &\sim \frac{1}{2\pi i} \int_{\beta_0 - i\infty}^{\beta_0 + i\infty} d\beta e^{\beta W} Z_{colorless}^{(I)}(\beta, V), \\
&\sim \frac{1}{2\pi i} \int_{\beta_0 - i\infty}^{\beta_0 + i\infty} d\beta e^{\beta W} e^{-\beta \mathcal{V}_{PVD M}(\beta; \Phi_0, \bar{\Phi}_0) - \beta \Omega_{q\bar{q}g}(\beta, V; \Phi_0, \bar{\Phi}_0)}, \\
&\sim \frac{e^{W_{PVD M}(\Phi_0, \bar{\Phi}_0)}}{2\pi i} \int_{\beta_0 - i\infty}^{\beta_0 + i\infty} d\beta e^{\beta W} e^{\frac{V}{\beta^3} a_{q\bar{q}g}(\Phi_0, \bar{\Phi}_0) + \frac{N_c N_f \Lambda^4}{4\pi^2} V \beta}, \\
&\sim \frac{e^{W_{PVD M}(\Phi_0, \bar{\Phi}_0)}}{2\pi i} \int_{\beta_0 - i\infty}^{\beta_0 + i\infty} d\beta e^{\beta W'} e^{\frac{V}{\beta^3} a_{q\bar{q}g}(\Phi_0, \bar{\Phi}_0)}, \tag{84}
\end{aligned}$$

where  $W' = W + \frac{N_c N_f \Lambda^4}{4\pi^2} V$  and

$$W_{PVD M}(\Phi_0, \bar{\Phi}_0) = \frac{1}{2} \log_e \left( 1 - 6\Phi_0 \bar{\Phi}_0 + 4 \left( \Phi_0^3 + \bar{\Phi}_0^3 \right) - 3 \left( \Phi_0 \bar{\Phi}_0 \right)^2 \right), \tag{85}$$

and

$$\begin{aligned}
a_{q\bar{q}g}(\Phi_0, \bar{\Phi}_0) &= 2N_f \int_0^\infty \frac{dx x^3}{2\pi^2} \left[ \frac{(\Phi_0 + 2\bar{\Phi}_0 e^{-x}) e^{-x} + e^{-3x}}{1 + (\Phi_0 + \bar{\Phi}_0 e^{-x}) e^{-x} + e^{-3x}} \right. \\
&\quad \left. + \frac{(\bar{\Phi}_0 + 2\Phi_0 e^{-x}) e^{-x} + e^{-3x}}{1 + (\bar{\Phi}_0 + \Phi_0 e^{-x}) e^{-x} + e^{-3x}} \right] + \omega_g \Phi_0 \bar{\Phi}_0. \tag{86}
\end{aligned}$$

In the limit of  $\Phi_0, \bar{\Phi}_0 \rightarrow 0$ , Eq.(86) is simplified to

$$\lim_{\Phi_0, \bar{\Phi}_0 \rightarrow 0} a_{q\bar{q}g}(\Phi_0, \bar{\Phi}_0) = \frac{N_f}{81} \left( \frac{7\pi^2}{60} \right). \tag{87}$$

Under the assumption of MIT bag model and in the limit of  $\Phi_0, \bar{\Phi}_0 \rightarrow 0$ , the extrapolation of the mass spectral density (I) is reduced to

$$\rho_{colorless}^{(I)}(m) \sim C \beta_{(I)}^{5/2} m^{-1/2} e^{bm}, \tag{88}$$

where  $m = W' + BV$  and  $B^{1/4} \sim 200 - 250$  MeV is the bag constant and

$$\begin{aligned}
\beta_{(I)} &= \left( \frac{N_f}{3^3} \frac{7\pi^2}{60} \frac{1}{3B} \right)^{1/4}, \\
b &= \beta_{(I)}, \\
C &= \frac{1}{2\sqrt{2\pi}} \left( \frac{4B}{\frac{N_f}{3^3} \frac{7\pi^2}{60}} \right)^{1/2}. \tag{89}
\end{aligned}$$

It is more appropriate to represent the large  $W$  limit in the term of asymptotic solution (II).

Under the assumption of solution (II), Hagedorn's density of states is approximated to

$$\lim_{W \rightarrow \infty} \rho_{colorless}^{(II)}(W, V) \sim \frac{1}{2\pi i} \int_{\beta_0 - i\infty}^{\beta_0 + i\infty} d\beta e^{\beta W} Z_{colorless}^{(II)}(\beta, V). \tag{90}$$

In the context of MIT bag model, Eq.(90) is reduced to

$$\rho_{colorless}^{(II)}(m) \sim C \beta_{(II)}^{\frac{3}{2}N_c^2+1} m^{-N_c^2/2} e^{bm}, \quad (91)$$

where

$$\begin{aligned} \beta_{(II)} &= \left( \frac{\frac{\pi^2}{15} (N_c^2 - 1) + \frac{7\pi^2}{60} N_c N_f}{3B} \right)^{1/4}, \\ b &= \beta_{(II)}, \\ C &= \frac{1}{2\sqrt{2\pi}} (4B)^{\frac{N_c^2}{2}} \frac{\left( \prod_{n=1}^{N_c-1} n! \right)}{\sqrt{N_c} (2\pi)^{\frac{N_c-1}{2}}} \frac{\left( \frac{1}{3} N_f + \frac{2\pi^2}{45} \frac{N_c^2-1}{N_c} \right)^{-\frac{N_c^2}{2} + \frac{1}{2}}}{\left( \frac{\pi^2}{15} (N_c^2 - 1) + \frac{7\pi^2}{60} N_c N_f \right)^{\frac{1}{2}}}. \end{aligned} \quad (92)$$

It is interesting to note that the mass spectral density for solution (I) does not lead to a deconfinement phase transition at Hagedorn's temperature while the system with mass spectral density (II) undergoes a first order deconfinement phase transition. For a system with two flavors (i.e.  $N_f = 2$ ) and  $B^{1/4} = 250$  MeV, Hagedorn's temperature for the deconfinement phase transition is reduced to  $T_H \sim 608$  MeV and 176 MeV for solutions (I) and (II), respectively. With smaller bag constant  $B^{1/4} = 200$  MeV, Hagedorn's temperature is reduced to  $T_H \sim 487$  MeV and 141 MeV for solutions (I) and (II), respectively. Hagedorn's temperature for the solution (II) is more acceptable than that for solution (I). When the exponent  $\alpha$  in  $\rho(m) \propto m^{-\alpha} e^{bm}$  runs over  $5/2 < \alpha \leq 7/2$ , Hagedorn matter undergoes a higher order phase transition while the system undergoes a first order phase transition for  $7/2 < \alpha$ . Therefore, GW-like phase transition is interpreted as an extrapolation of the discrete mass spectrum of the conventional hadronic states that are found in the data book [31] to Hagedorn states (i.e. super massive hadronic states) that are represented by the bootstrap-like models. In this context, the deconfinement phase transition to QGP takes place at Hagedorn's temperature. In this sense, GW-like transition is a hadronic mechanism that produces meta-stable super-massive hadronic states (known as Hagedorn states) below the deconfinement phase transition to QGP. Finally, it should be noted that the regularization procedure for VanderMonde's number of states reduces the spectral density to

$$\begin{aligned} \rho_{colorless}^{(II)}(m) &\propto m^{-\alpha} e^{bm}, \\ &\propto m^{-\left(\frac{\gamma_{reg}}{2} (N_c^2-1) + \frac{1}{2}\right)} e^{bm}. \end{aligned} \quad (93)$$



Eq.(93) demonstrates that  $\gamma_{reg}$  may be related to the bag's volume fluctuation. It is reduced to  $\gamma_{reg} = 1$  for a bag with a sharp surface boundary. The cases  $\gamma_{reg} < 1$  and  $\gamma_{reg} > 1$  correspond to the expanding (dilute) and squeezing (compressed) bags, respectively. The case  $\gamma_{reg} < 1$  is related to the bag with an extended surface boundary. The exponent  $\alpha$  is reduced to  $\frac{9}{2}$  and  $\frac{3}{2}$  for  $\gamma_{reg} = 1$  and  $\gamma_{reg} = \frac{1}{4}$ , respectively.

## V. DISCUSSION AND CONCLUSION

We have considered the canonical ensemble for colorless quark and gluon blob. The colorless quark and gluon blobs emerge as meta-stable Hagedorn states in the relativistic heavy ion collisions. These colorless states (i.e. Hagedorn states) significantly enrich the deconfinement phase transition diagram. Their production signature may mix and be confused with QGP. In order to make the discussion simple, at first we neglect the effect of chiral field and simply assume massless 2-flavors in order to simplify the analysis of GW-like phase transition. The low-lying energy solution, namely, solution (I), is determined by non-Gaussian stationary point method for Polyakov loop parameters  $(\Phi, \bar{\Phi})$  as defined by Eq.(33). The high-lying energy solution, namely, solution (II), is determined by the Gaussian saddle point approximation. The assumption is that the non-Gaussian stationary points of solution (I) turn to Gaussian saddle points in solution (II). The solution (II) is introduced by Eq.(34). Furthermore, the exact numerical solution is considered by evaluating the exact numerical integration over the fundamental gauge fields  $\theta_1$  and  $\theta_2$  with the invariance Haar measure which is given by Eq.(27).

Fig. 1 depicts the quantity  $\frac{T}{V} \log_e Z_{colorless}(T, V)$  which represents the *negative* Helmholtz free energy density vs  $T$  for quark and gluon blob with various volumes  $R = 0.57, R = 0.71, R = 0.82$  and  $R = 0.90$  fm. It is shown that solution (I) matches exact numerical solution below GW-threshold temperature and then it deviates from the exact one when the temperature reaches and exceeds GW-threshold point while solution (II) converges to the exact numerical solution as temperature approaches GW-ultimate point until it fits precisely the exact one as temperature exceeds that point. Therefore, solution (I) is the correct asymptotic solution for any temperature below GW-threshold point while solution (II) is the correct asymptotic solution for any temperatures above GW-ultimate point. Furthermore, it seems that neither solution (I) nor solution (II) fits correctly the exact numerical solution

over an extended GW-like point domain which covers the interval between GW-threshold and ultimate points. Evidently, the interpolation of both solutions (I) and (II) over the interval between GW-threshold and ultimate points fits the exact numerical solution. This makes a smooth transition from solution (I) to solution (II) over an extended GW-like point interval. The domain between threshold and ultimate points (i.e. over the extended GW-like point interval) is reduced to a single point in the limit  $N_c \rightarrow \infty$  but a finite coupling constant  $g N_c^2$ . Therefore, the analytical solution is modified *smoothly* from solution (I) to solution (II) over the extended GW-point interval. This implies that low-lying and high-lying mass spectra remain in mutual exchange reaction over the extended GW-point interval. The high-lying energy solution (II) significantly deviates from the exact solution at temperature below GW-threshold and then turns to converge to the exact one as the temperature approaches GW-ultimate point and then remains in an excellent match as the temperature increases beyond GW-ultimate point. On the other hand, the low-lying energy solution (I) matches the exact numerical solution precisely for temperature below GW-threshold and then it starts to deviate significantly from the exact one when the temperature exceeds GW-threshold. This deviation is significant as temperature increases above GW-ultimate point. The *smooth* modification in the solution's analytic behavior through the extended GW-point interval clearly implies that Hagedorn states emerge as meta-stable states over an extended GW-point interval with mutual and exchange chemical reaction between the high-lying and low-lying hadronic states. The exchange reaction clarifies the difficulty to detect Hagedorn states, GW-like transition and the subsequent confusion with the deconfinement phase transition.

The order parameter  $\Phi_0$  for solution (I) vs temperature is depicted in Fig. 2 with various volumes of colorless quark and gluon bags. The order parameter  $\Phi_0$  is simply the stationary point that projects the color singlet state under the assumption of solution (I). The order parameter  $\Phi_0$  is found very small at low temperatures and this is because of the strong confinement. This implies a reduced gluonic component for hadronic states at low temperatures since  $\Phi_0$  and  $\bar{\Phi}_0$  correspond the gluon condensates. Furthermore, when the system is heated up, the value of  $\Phi_0$  increases and approaches its restoration value from below but remains  $\Phi_0 < 1$ . The  $\Phi_0$ 's asymptotic restoration indicates loose confinement states or meta-stable bubbles. Furthermore,  $\Phi_0$  increases from  $\Phi_0 \approx 0^+$  to the restoration value  $\Phi_0 \approx 1^-$  within the extended GW-point interval as the asymptotic solution switches from (I) to (II). Although, GW-like phase transition from strong coupling to weak cou-

pling has been extensively considered in the context of large- $N_c$  limit, it is evident that GW-like phase transition persists to exist even in QCD with  $N_c = 3$  but with different analytical behavior. The GW-like phase transition in QCD is not a conventional confinement/deconfinement phase transition but is the Hagedorn's production threshold. This can be understood in the term of micro-canonical ensemble and the consideration of gas of Hagedorn states. The micro-canonical ensemble of solution (II) is the mass spectral density of Hagedorn states where GW-like point corresponds the Hagedorn's mass threshold (i.e.  $m_{threshold} \sim 2$  GeV). Therefore, the present results suggest that GW-like phase transition persists to exist in QCD and, subsequently, the Polyakov loop restoration turns to be the onset of GW-like phase transition or semi-QGP and the existence of Hagedorn states where Hagedorn states are produced in the hadronic phase. This interpretation, definitely, implies that the Polyakov loop restoration is not the deconfinement's order parameter as has been suggested in some models [1] but the abundant production of (meta-stable) Hagedorn states below Hagedorn's temperature. This conclusion is also true for PNJL model where the  $\sigma$ -chiral field is considered explicitly and self-consistently in the calculation. Fig.3 displays the *negative* Helmholtz free energy vs temperature with various volumes. The general situation looks very similar to Fig. 1. The solution (I) matches the exact numerical one for temperature below GW-threshold. When the temperature exceeds GW-threshold point, solution (I) starts to deviate significantly above the exact one. It continues to deviate above the exact numerical one as the temperature increases. On the other hand, the high-lying energy solution, namely solution (II), has a hidden valley that deviates significantly from the exact numerical one at low temperature as far the temperature remains below GW-ultimate limit. This valley emerges due to the unphysical oscillatory behavior of the Gaussian saddle point approximation below GW-like point. Nonetheless, solutions (I) and (II) intersect with each others at GW-threshold temperature below GW-ultimate temperature. When the temperature increases and reaches GW-ultimate point, solution (II) converges to and matches precisely the exact numerical one. Furthermore, as the temperature increases and exceeds GW-ultimate point, solution (II) converges to exact numerical one and remains in an excellent agreement. Therefore, evidently there is a switch from solution (I) to solution (II) within the extended GW-point interval. Nevertheless, the extended GW-point interval is ambiguous in heavy ion collisions as far neither solution (I) nor solution (II) fits the exact one while their interpolation seems to fit to the exact numerical solution. The importance

of this mechanism is that it may shed the light on the existence of (meta-) Hagedorn states and their production as super-massive hadronic states (i.e.  $m_H > 2$  GeV). The extended GW-point interval (i.e. the interval between the threshold and ultimate points) is very sensitive to the fireball's volume. For instance, the extended GW-point interval is extended from  $T_{min}$  to  $T_{max}$  ( $\sim 181 - 291$  MeV) for bag's radius  $R = 0.57$  fm. The extended GW-point interval is significantly reduced and turns to  $\sim 119 - 184.5$  MeV for bag's radius  $R = 0.90$  fm. Hence, Hagedorn states turn to be of the size of QGP (i.e.  $R \geq 0.90$  fm) for temperature close to the deconfinement one (i.e.  $T \approx 184.5$  MeV). Furthermore, Hagedorn states with size  $R = 0.57$  fm are likely to be produced at rather high temperature  $T_{max} = 291$  MeV while large Hagedorn states are produced at lower temperatures. This unusual behavior makes more difficult to detect Hagedorn states as far they emerge as super-massive, gluonic rich and meta-stable states with the size order of QGP. The large (volume and mass) Hagedorn states can be confused and mixed with a true deconfinement phase transition's signature. The (super-)massive Hagedorn states can be developed as droplets of semi-quark-gluon plasma in colorless states. Fig. 4 depicts the order parameter  $\Phi_0$  for solution (I) vs temperature with various volumes. The restoration of Polyakov loop  $\Phi_0$  likely takes place over the extended GW-point interval (i.e. between GW-threshold and ultimate points). When  $T$  approaches GW-threshold,  $\Phi_0$  (and  $\bar{\Phi}_0$ ) starts its significant restoration process. Furthermore, when  $T$  exceeds GW-ultimate point  $\Phi_0$  turns to be almost restored from below (i.e.  $\Phi_0 \leq 1$ ). This behavior hints that the non-Gaussian stationary point approximation fails at temperature above GW-threshold. Subsequently, the non-Gaussian stationary point approximation is converted to Gaussian saddle point approximation.

The effective chiral field  $G\sigma$  vs  $T$  with various volumes is displayed in Fig. 5. The  $\sigma$ -chiral mean field is considered self-consistently in the frame work of solutions (I) and (II) as well as the exact numerical solution. The results show clearly that the chiral restoration likely takes place within an extend GW-point interval but below GW-ultimate point. Furthermore, the solution (II)'s chiral restoration takes place before that one for solution (I). This implies that chiral restoration likely takes place within an extended GW-point interval above GW-threshold point but below GW-ultimate point. The both solutions (I) and (II) fail to locate the precise position of chiral restoration. This deficit is understood by realizing that extrapolation of solution (I) or (II) is not the correct asymptotic solution over the extended GW-point interval. Furthermore, the chiral restoration of the exact numerical solution usu-

ally occurs on the right hand side of solutions (I) and (II) but below GW-ultimate point. This can be interpreted as exchange reaction and smooth transition between the low-lying and high-lying hadronic states over the extended GW-point interval. The chiral restoration takes place within an extended GW-point interval but far away from GW-ultimate point for small fireball ( $R \sim 0.57$  fm). The restoration point approaches GW-ultimate point from below as the fireball size increases. Hence, Hagedorn threshold production takes place within an extended GW-point interval. The results demonstrate that the (meta-) Hagedorn states are chirally restored above GW-ultimate.

The results suggest that there is a new class of phase transition in nuclear matter in particular in the hadronic sector. The Hadronic phase turns to be smoothly dominated by a gas of colorless quark-gluon bags through the extended GW-point interval. This mechanism can be understood in the term of Hagedorn states. The size of Hagedorn's bags continue to grow up until Hagedorn's temperature is reached. When Hagedorn's temperature is reached, the system undergoes a deconfinement phase transition to QGP. The finite volume colorless states have been suggested before by Elze, Greiner and Rafelski [18–22]. This picture has been extended to the gas of bags. The results also suggest a possible production of large (meta-) colorless quark-gluon droplets of the size order of quark-gluon plasma  $R \geq 0.90$  fm at  $T \leq 184.5$  MeV (in the case of a single droplet analysis). The smaller Hagedorn states are produced at much higher temperatures. For instance bags with  $R \sim 0.57$  fm are produced at  $T \sim 291$  MeV. This supports that small size hadronic states belong to the low-lying hadronic mass spectrum rather than high-lying hadronic mass spectrum. In the case of gas of bags, the analysis can be extended using Hagedorn's density of states that is derived from the micro-canonical ensemble. This indicates that the nuclear matter undergoes smooth transition from low-lying mass spectrum to (meta-) Hagedorn states (or even semi-QGP) rather than directly to true deconfined QGP. The deconfinement phase transition takes place at Hagedorn's temperature. The production of colorless QG-fireballs enriches the nuclear phase transition diagram significantly. This mechanism opens a window to produce (meta-)stable colorless super-massive QG-droplets at the size of order of QGP. Finally, the signature of deconfined QGP in the heavy ion collisions may be confused and/or mixed with the gas of colorless QG-bags or semi-QGP.

## Acknowledgments

This work was supported by Helmholtz International Centre for FAIR within the framework of the LOEWE program (Landesoffensive zur Entwicklung Wissenschaftlich-Ökonomischer Exzellenz) launched by the State of Hesse is acknowledged. One of us (IZ) thanks C. Sasaki, R. Pisarski and E. Witten for the discussion.

- 
- [1] K. Fukushima, Phys.Lett. **B591**, 277 (2004), arXiv:hep-ph/0310121 [hep-ph] .
  - [2] A. Gocksch and R. D. Pisarski, Nucl.Phys. **B402**, 657 (1993), arXiv:hep-ph/9302233 [hep-ph] .
  - [3] K. Fukushima, Phys.Rev. **D77**, 114028 (2008), arXiv:0803.3318 [hep-ph] .
  - [4] C. Ratti, M. A. Thaler, and W. Weise, Phys.Rev. **D73**, 014019 (2006), arXiv:hep-ph/0506234 [hep-ph] .
  - [5] S. Roessner, C. Ratti, and W. Weise, Phys.Rev. **D75**, 034007 (2007), arXiv:hep-ph/0609281 [hep-ph] .
  - [6] T. Sasaki, Y. Sakai, H. Kouno, and M. Yahiro, Phys.Rev. **D82**, 116004 (2010), arXiv:1005.0910 [hep-ph] .
  - [7] Y. Sakai, K. Kashiwa, H. Kouno, and M. Yahiro, Phys.Rev. **D77**, 051901 (2008), arXiv:0801.0034 [hep-ph] .
  - [8] B.-J. Schaefer, M. Wagner, and J. Wambach, Phys.Rev. **D81**, 074013 (2010), arXiv:0910.5628 [hep-ph] .
  - [9] B.-J. Schaefer, J. M. Pawłowski, and J. Wambach, Phys.Rev. **D76**, 074023 (2007), arXiv:0704.3234 [hep-ph] .
  - [10] M. Ciminale, R. Gatto, N. Ippolito, G. Nardulli, and M. Ruggieri, Phys.Rev. **D77**, 054023 (2008), arXiv:0711.3397 [hep-ph] .
  - [11] H. Abuki, R. Anglani, R. Gatto, G. Nardulli, and M. Ruggieri, Phys.Rev. **D78**, 034034 (2008), arXiv:0805.1509 [hep-ph] .
  - [12] H. Abuki, M. Ciminale, R. Gatto, G. Nardulli, and M. Ruggieri, Phys.Rev. **D77**, 074018 (2008), arXiv:0802.2396 [hep-ph] .
  - [13] H. Abuki, M. Ciminale, R. Gatto, and M. Ruggieri, Phys.Rev. **D79**, 034021 (2009),

- arXiv:0811.1512 [hep-ph] .
- [14] I. Zakout and C. Greiner, (2010), arXiv:1002.3119 [nucl-th] .
  - [15] A. Andronic, D. Blaschke, P. Braun-Munzinger, J. Cleymans, K. Fukushima, *et al.*, Nucl.Phys. **A837**, 65 (2010), arXiv:0911.4806 [hep-ph] .
  - [16] E. Brezin, C. Itzykson, G. Parisi, and J. B. Zuber, Commun. Math. Phys. **59**, 35 (1978).
  - [17] D. J. Gross and E. Witten, Phys. Rev. **D21**, 446 (1980).
  - [18] H. T. Elze and W. Greiner, Phys. Lett. **B179**, 385 (1986).
  - [19] H. T. Elze, D. E. Miller, and K. Redlich, Phys. Rev. **D35**, 748 (1987).
  - [20] H. T. Elze, W. Greiner, and J. Rafelski, Phys. Lett. **B124**, 515 (1983).
  - [21] H.-T. Elze, W. Greiner, and J. Rafelski, Z. Phys. **C24**, 361 (1984).
  - [22] H. T. Elze and W. Greiner, Phys. Rev. **A33**, 1879 (1986).
  - [23] C. Spieles, H. Stoecker, and C. Greiner, Phys. Rev. **C57**, 908 (1998), arXiv:hep-ph/9708280 .
  - [24] I. Zakout, C. Greiner, and J. Schaffner-Bielich, Nucl. Phys. **A781**, 150 (2007), arXiv:nucl-th/0605052 .
  - [25] I. Zakout and C. Greiner, Phys. Rev. **C78**, 034916 (2008), arXiv:0709.0144 [nucl-th] [nucl-th] .
  - [26] M. I. Gorenstein, S. I. Lipskikh, V. K. Petrov, and G. M. Zinovev, Phys. Lett. **B123**, 437 (1983).
  - [27] G. Auberson, L. Epele, G. Mahoux, and F. R. A. Simao, J. Math. Phys. **27**, 1658 (1986).
  - [28] M. L. Mehta, *Random Matrices and the Statistical Theory of Energy Levels* (Academic Press Inc, 1967).
  - [29] This point has been brought to the attention of the authors by C. Sasaki.
  - [30] This point has been brought to the attention of the authors by R. Pisarski.
  - [31] C. Amsler *et al.* (Particle Data Group), Phys. Lett. **B667**, 1 (2008).
  - [32] This point has been brought to the attention of the authors by C. Sasaki
  - [33] This point has been brought to the attention of the authors by R. Pisarski.

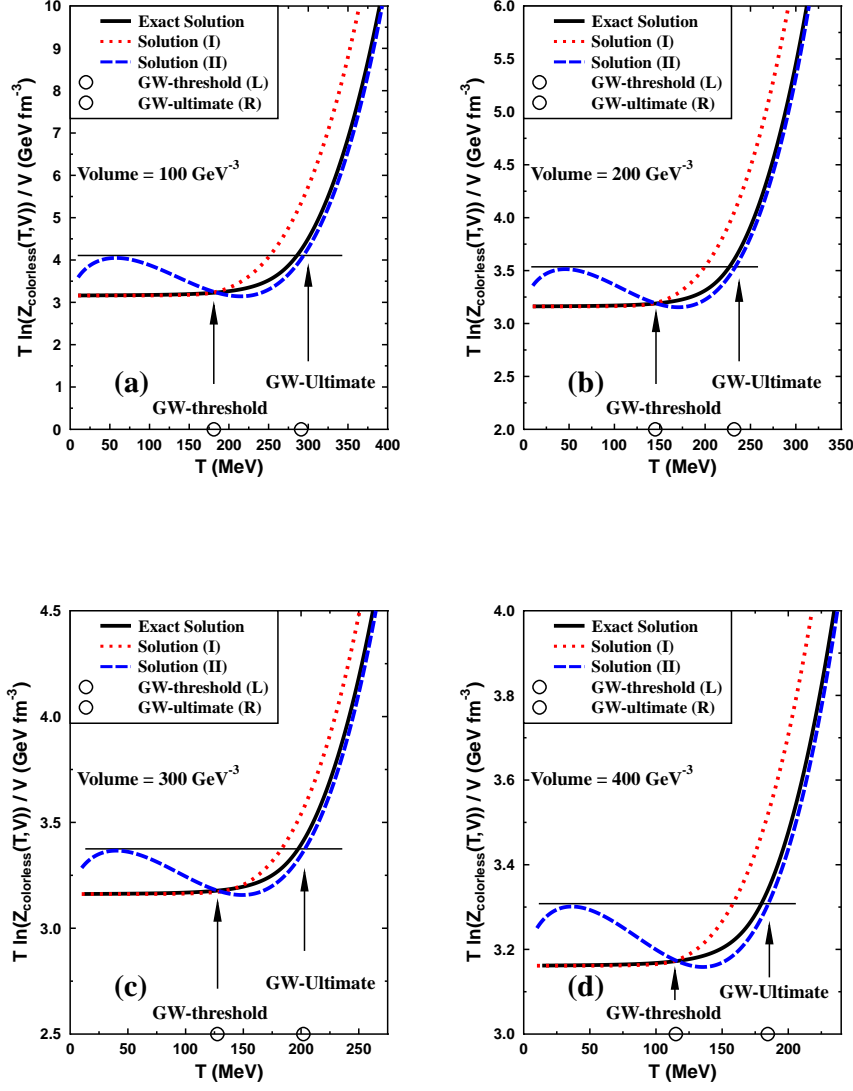


FIG. 1: (Color online) The *negative* Helmholtz free energy density  $\frac{T}{V} \log_e Z_{\text{colorless}}(T, V)$  for the low-lying energy (I) and high-lying energy (II) solutions and the exact one (i.e. the phase transition solution (I)  $\rightarrow$  (II) between GW-threshold and ultimate points) vs temperature. No chiral field is considered. The GW-threshold and ultimate points are shown as circles in the  $T$ -axis. The results for volumes 100, 200, 300 and 400  $\text{GeV}^{-3}$  (i.e.  $R = 0.57, 0.71, 0.82$  and  $0.90$  fm) are displayed respectively in (a), (b), (c) and (d), respectively.



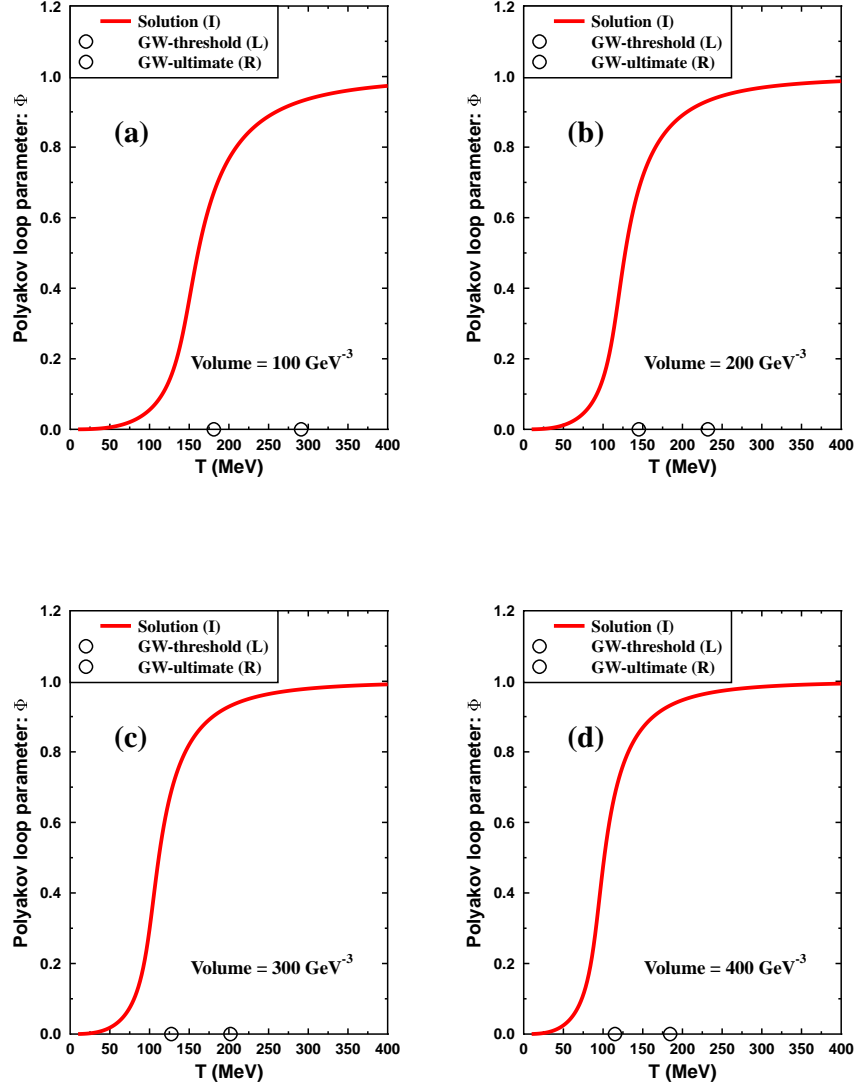


FIG. 2: (Color online) The Polyakov loop (triality) parameter  $\Phi$ , the order parameter of solution (I), vs temperature with various bag's volume. The chiral field is not included. (a)  $V = 100 \text{ GeV}^{-3}$ . (b)  $V = 200 \text{ GeV}^{-3}$ . (c)  $V = 300 \text{ GeV}^{-3}$ . (d)  $V = 400 \text{ GeV}^{-3}$ .

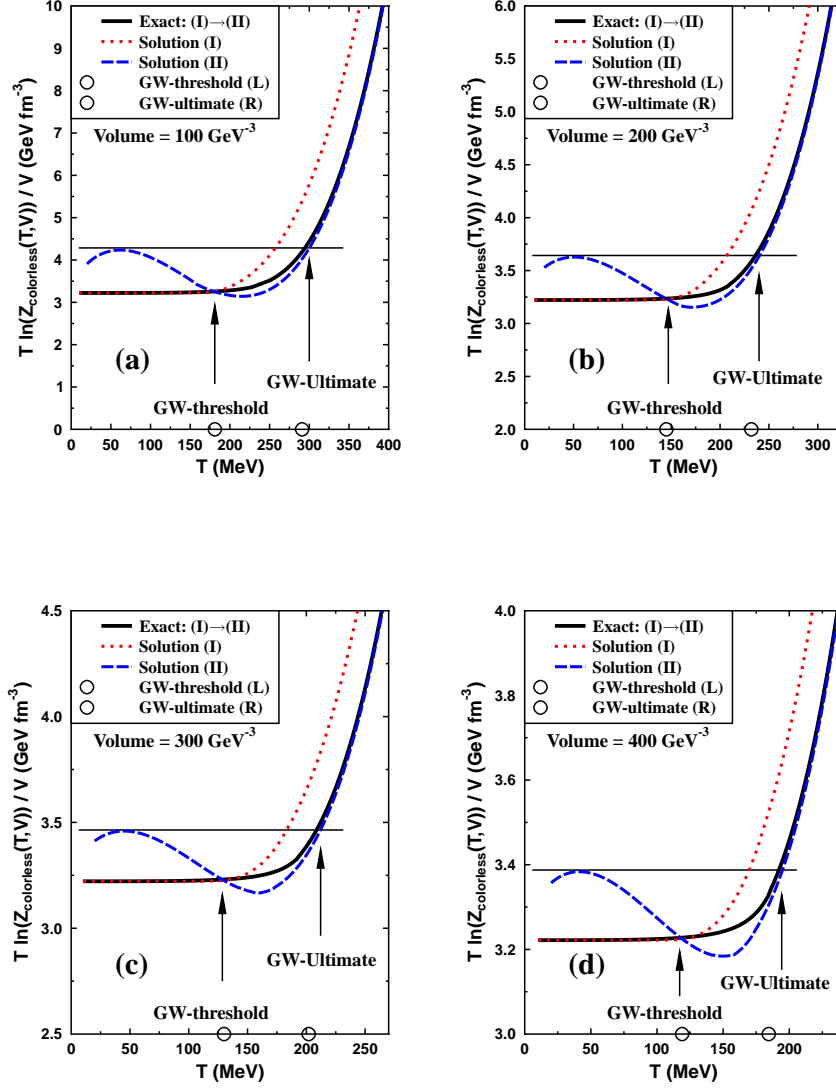


FIG. 3: (Color online) The *negative* Helmholtz free energy density  $\frac{T}{V} \log_e Z_{\text{colorless}}(T, V)$  for the low-lying energy (I) and high-lying energy (II) solutions and exact one vs temperature. The  $\sigma$ -chiral mean field is included simultaneously in the calculation. The GW-threshold and ultimate points are shown as circles in the  $T$ -axis. (a)  $V = 100 \text{ GeV}^{-3}$  ( $R = 0.57 \text{ fm}$ ). (b)  $V = 200 \text{ GeV}^{-3}$  ( $R = 0.71 \text{ fm}$ ). (c)  $V = 300 \text{ GeV}^{-3}$  ( $R = 0.82 \text{ fm}$ ). (d)  $V = 400 \text{ GeV}^{-3}$  ( $R = 0.90 \text{ fm}$ ).

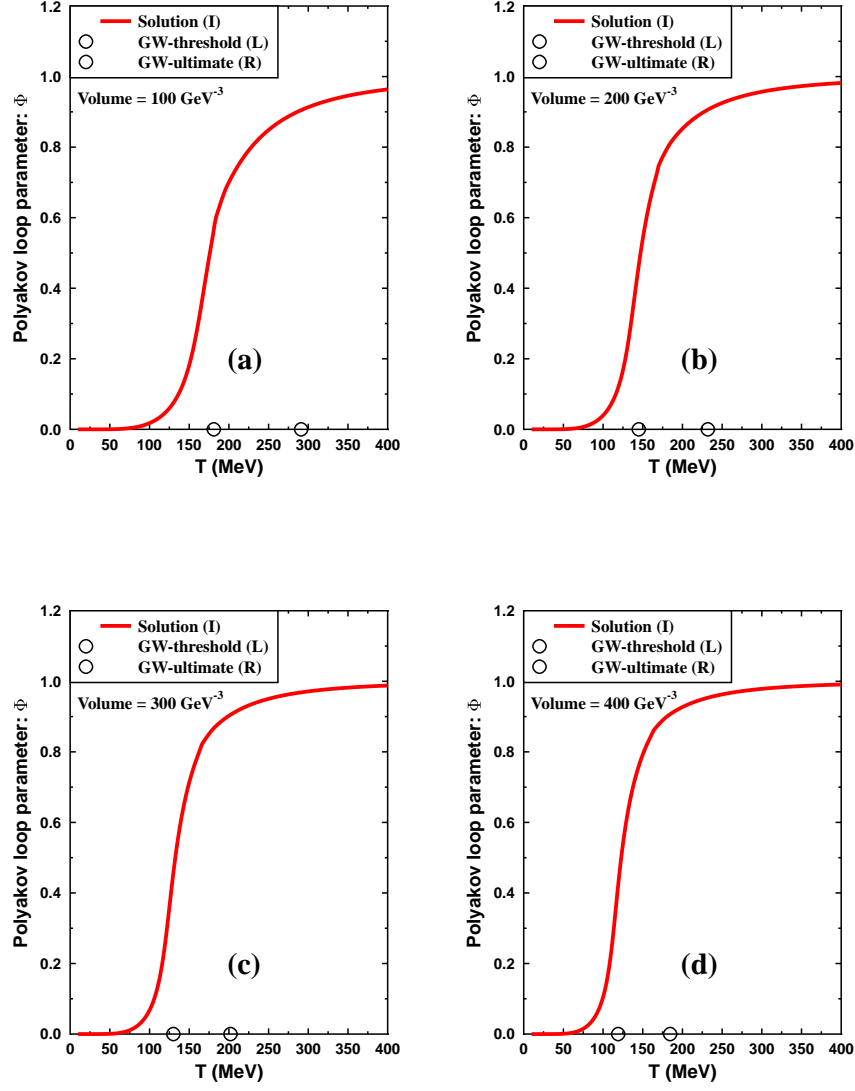


FIG. 4: (Color online) The Polyakov loop (triality) parameter  $\Phi$ , the order parameter of solution (I), vs temperature with various bag's volume. The  $\sigma$ -chiral mean field is included simultaneously in the calculation. (a)  $V = 100 \text{ GeV}^{-3}$ . (b)  $V = 200 \text{ GeV}^{-3}$ . (c)  $V = 300 \text{ GeV}^{-3}$ . (d)  $V = 400 \text{ GeV}^{-3}$ .

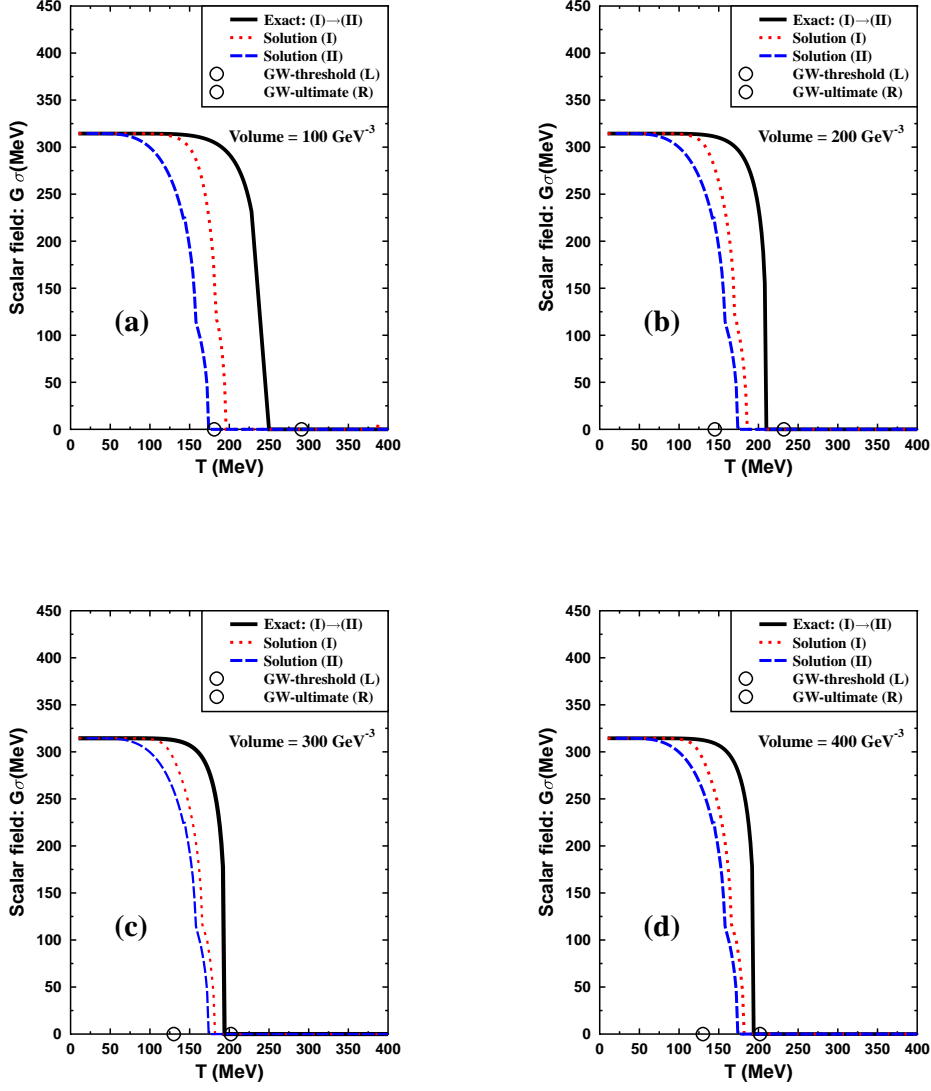


FIG. 5: (Color online) The chiral mass  $G\sigma$  vs temperature for the low-lying (I) and high-lying (II) energy solutions and the exact one (i.e. the phase transition solution (I)  $\rightarrow$  (II) between GW-threshold and ultimate points) with various bag's volume. The  $\sigma$ -chiral mean field and Polyakov loops are included simultaneously in the calculation. (a)  $V = 100\text{GeV}^{-3}$ . (b)  $V = 200\text{GeV}^{-3}$ . (c)  $V = 300\text{GeV}^{-3}$ . (d)  $V = 400\text{GeV}^{-3}$ .